UNIVERSITY OF AZUAY

Postgraduate Department

Master in Environmental Management

Assessment of Different Methodologies to Estimate Daily Reference Evapotranspiration in Páramo Ecosystems, Azuay Province

---

A thesis submitted in partial fulfillment of the requirements to obtain the degree of:

Master in Environmental Management

Author:

Juan Andrés Pinos Flores

Director:

MSc. Aleksandr Khachatryan

Cuenca, Ecuador

January, 2018

UNIVERSIDAD DEL AZUAY

Departamento de Posgrados

Maestría en Gestión Ambiental

Evaluación de Diferentes Metodologías para Estimar la Evapotranspiración Diaria de Referencia en Ecosistemas de Páramo, Provincia del Azuay

---

Trabajo de graduación previo a la obtención del título de:

Magíster en Gestión Ambiental

Autor:

Juan Andrés Pinos Flores

Director:

Msc. Aleksandr Khachatryan

Cuenca, Ecuador

Enero, 2018

Acknowledgements

First and foremost, I would like to thank my supervisor, Aleksandr Khachatryan for his guidance and expertise throughout this project, as well as his support and encouragement for helping me through it. I would like to thank Gustavo Chacón for his support as well, in addition to helping me to improve the writing of the thesis. Thank you also to Juan José Contreras and Eric Webster, for their input in shaping this thesis into its final product.

Dedication

This thesis is dedicated to my family, every one of them, for all of their love and support in getting me to this point.

Assessment of Different Methodologies to Estimate Daily Reference Evapotranspiration in Páramo Ecosystems, Azuay Province

Juan A. Pinos, Aleksandr Khachatryan, Gustavo Chacón, Danilo Minga

To be submitted to PLoS One

Abstract

Evapotranspiration (ET) is poorly studied in very-wet regions in spite of its outstanding importance in water management. This study aimed at estimating daily reference ET (ETo) in páramo ecosystems in the Andean Highlands, Southern Ecuador to compare it to the FAO 56 P-M method. Available data of two weather stations: Toreadora (2013-2016 period) and Zhurucay (2014 period) were used to assess the performances of 30 predictive models (21 empirical = radiation-, temperature-, combination- and mass transfer-based; 8 artificial neural networks-ANNs, and 1 multivariate adaptive regression splines-MARS). A simple statistical analysis was carried out (MBE, MAE, RMSE). An initial Random Forests analysis was developed to measure the relative importance of weather variables. These results were used to assemble ANNs with combinations of weather variables and the obtained smallest possible number of inputs. MARS helped to develop the REMPE equation using the solar radiation and the relative humidity as main inputs. The results showed that ANNs were the most accurate models to estimate ETo; however, the combination-based equations had the best performances. These were followed by radiation-based, temperature-based and mass transfer-based equations. A calibration method improved performances of most of the empirical models, and worsen those of the remaining models. These results were explained by the distribution of calibration radiuses for each equation. The mass transfer-based, and the REMPE equations exhibited the worst performances, and it is suggested that these equations should not be used in super-humid environments. These results represent a practical and helpful tool to facilitate decisions, and the selection of the best model when available data is scarce.

Keywords: Water resources, Climatic description, Reference ET, Penman-Monteith method, Prediction models comparison

Evaluación de Diferentes Metodologías para Estimar la Evapotranspiración Diaria de Referencia en Ecosistemas de Páramo, Provincia del Azuay

Juan A. Pinos, Aleksandr Khachatryan, Gustavo Chacón, Danilo Minga

Para ser enviado a PLoS One

Resumen

La evapotranspiración (ET) ha sido poco estudiada en regiones muy húmedas, a pesar de su destacada importancia en la gestión del agua. El objetivo de este estudio fue estimar la ET diaria de referencia (ETo) en ecosistemas de páramo en el altiplano andino, sur de Ecuador, para compararla con el método FAO 56 P-M. Datos disponibles de dos estaciones meteorológicas: Toreadora (período 2013-2016) y Zhurucay (período 2014) se utilizaron para evaluar el rendimiento de 30 modelos predictivos (21 empíricos basado en= radiación, temperatura, combinación y transferencia de masa; 8 redes neuronales artificales-RNAs y 1 splines de regresión adaptativa multivariante-MARS). Se realizó un análisis estadístico simple (MBE, MAE, RMSE). Se desarrolló un análisis inicial de Random Forests para medir la importancia relativa de las variables climáticas. Estos resultados se usaron para ensamblar las RNAs en combinaciones de las variables climáticas y con el menor número posible de entradas. MARS ayudó a desarrollar la ecuación de REMPE usando la radiación solar y la humedad relativa como entradas principales. Los resultados mostraron que las RNAs son los modelos más precisos para estimar ETo; sin embargo, las ecuaciones basadas en combinaciones también obtuvieron buenos rendimientos. Estos fueron seguidos por ecuaciones basadas en radiación, basadas en temperatura y basadas en transferencia de masa. Un método de calibración mejoró el rendimiento de la mayoría de los modelos empíricos y empeoró los de los modelos restantes. Estos resultados se explicaron por la distribución de radios de calibración para cada ecuación. Las ecuaciones basadas en la transferencia de masa y REMPE exhibieron los peores resultados, y se sugiere que estas ecuaciones no se deben ser utilizadas en entornos super-húmedos. Estos resultados representan una herramienta práctica y útil para facilitar la toma de decisiones y la selección del mejor modelo cuando los datos disponibles son escasos.

Palabras clave: Recursos hídricos, Descripción climática, ET de referencia, Método de Penman-Monteith, Comparación de modelos de predicción.

TABLE OF CONTENTS

1. Introduction 1

1.1 The Andean páramos 1

1.2 Evapotranspiration 1

2. Material and methods 4

2.1 Study area 4

2.2 Methods for estimating reference evapotranspiration 5

2.3 Validation and calibration of simplified methods 11

2.4 Variable importance measured with random forests 11

2.5 Artificial neural networks 12

2.6 Multivariate adaptive regression splines (MARS) 13

2.7 Model comparison analysis 14

3. Results and Discussion 15

3.1 Analyses of influential weather variables and model performance 15

3.2 Comparison of methodologies for ETo estimation 15

3.2.1 Empirical models 18

3.2.2 Calibration of empirical models 19

3.2.3 Artificial neural networks models 20

3.2.4 MARS model 21

3.2.5 Annual reference evapotranspiration 21

4. Conclusions 23

5. References 24

LIST OF FIGURES

Figure 1. Evapotranspiration process 2

Figure 2. Weather variables that influence the ET process 2

Figure 3. Calculation process of reference crop evapotranspiration (ETo), and actual crop evapotranspiration under standard conditions (ETc) 3

Figure 4. Locations of automatic weather stations 4

Figure 5. Example of maximum and minimum relative humidity pattern (2015 period of Toreadora weather station) 15

Figure 6. Graphical representation of statistical performance of the different ETo estimation methods versus FAO 56 P-M model. A) Toreadora weather station; B) Zhurucay weather station 16

Figure 7. Graphical representation of statistical performance of the different calibrated ETo estimation methods versus FAO 56 P-M model. A) Toreadora weather station; B) Zhurucay weather station 17

Figure 8. Box plot of calibration radiuses (cr) for 21 empirical models. The median (center line), interquartile range (25% to 75%) (box) and interquartile range (0-25% and 75-100%) multiple to a factor (1.5) (whiskers) 19

Figure 9. Annual ETo estimated from original empirical models. A) data from Toreadora weather station; B) data from Zhurucay weather station 21

Figure 10. Annual ETo estimated from different calibrated methods. A) data from Toreadora weather station; B) data from Zhurucay weather station........................... 22

LIST OF TABLES

Table 1. Selected models to estimate potential daily evapotranspiration with their reference, formula, and parameterization 9

Table 2. Variable importance of FAO 56 P-M equation inputs applying random forests 12

Table 3. Inputs for the application of each ANN 13

Table 4. Summary of training and cross validation processes of the evaluated ANNs 20

LIST OF APPENDICES

Appendix 1. Daily ETo estimations of temperature-based models. Temporal comparison against the reference model (FAO 56 P-M) for both weather stations 30

Appendix 2. Daily ETo estimations of radiation-based models. Temporal comparison against the reference model (FAO 56 P-M) for Toreadora weather station 31

Appendix 3. Daily ETo estimations of radiation-based models. Temporal comparison against the reference model (FAO 56 P-M) for Zhurucay weather station 32

Appendix 4. Daily ETo estimations of combination-based models. Temporal comparison against the reference model (FAO 56 P-M) for both weather stations 33

Appendix 5. Daily ETo estimations of mass transfer-based models. Temporal comparison against the reference model (FAO 56 P-M) for Toreadora weather station 34

Appendix 6. Daily ETo estimations of mass transfer-based models. Temporal comparison against the reference model (FAO 56 P-M) for Zhurucay weather station 35

Appendix 7. Daily ETo estimations of ANN models. Temporal comparison against the reference model (FAO 56 P-M) for Toreadora weather station 36

Appendix 8. Daily ETo estimations of ANN models. Temporal comparison against the reference model (FAO 56 P-M) for Zhurucay weather station 37

Appendix 9. Daily ETo estimations of REMPE model. Temporal comparison against the reference model (FAO 56 P-M) for both weather stations 38

Appendix 10. Statistical performance of ETo estimation methods versus FAO 56 P-M model for daily ETo estimation with data from the 2016 period (Toreadora weather station)... 39

Appendix 11. Statistical performance of ETo estimation methods versus FAO 56 P-M model for daily ETo estimation with data from the 2014 period (Zhurucay weather station)... 41

1. Introduction

1.1 The Andean páramos

The Andean mountain range crosses the western fringe of South America, including Ecuador. The Ecuadorian highlands represent 34% of the area of the country which is located along the inter-Andean alley (Célleri & Feyen, 2009). One of the main ecosystems found in this mountainous area is the páramo. The Andean páramos consist of accidental, mostly glacier formed valleys and plains with a large variety of lakes, peat bogs and wet grasslands intermingled with shrub lands and low-statured forest patches. The total area covered by páramo is estimated between 35000 (Hofstede et al., 2003) and 77000 km^2 (Dinerstein et al., 1995). This discrepancy is primarily due to uncertainties in the lower limit of the páramo. The natural forest limit is severely altered by human activity (logging, intensive grazing), which makes the difference between natural and artificial grasslands difficult to distinguish (Buytaert et al., 2006). The Andean páramo is an intertropical montane ecosystem located generally between altitudes of 3000 m to the line of perpetual snows, approximately 4300 m. In Ecuador, the altitude of 3500 m is commonly used as the lower limit, but the geological, climatic and anthropogenic conditions make this limit vary a lot, and that are sometimes páramos from 2800 m, especially in the south of the country; or closed forests up to over 4000 m (Medina & Mena, 2001).

In Ecuador, the páramo covers around 1250000 ha, that is, approximately 6% of the national territory (Medina & Mena, 2001). The páramo features a typical tropical high mountain climate (cold and humid). Due to its location close to the equator, the daily solar radiation is almost constant throughout the year. Intraday temperature variations of more than 20 °C are common (“summer every day and winter every night”) (Buytaert et al., 2006). The precipitation can vary greatly, from values lower than 700 mm to more than 3000 mm (Luteyn, 1992), with some extremes in limited areas, up to 6000 mm (Rangel, 2000). The páramo presents very particular hydrological characteristics. Water production in small watersheds can exceed half of the total rainfall. This is explained by the soils with high contents of organic matter (great water retention capacity), by the low rates of evapotranspiration due to the climate and the absence of a marked dry season (Padrón, 2013).

1.2 Evapotranspiration

The monitoring and modeling of land surface and vegetation processes is an essential tool for the assessment of water and carbon dynamics of terrestrial ecosystems. Evapotranspiration (ET) is the simultaneous process of transferring water -originating from a wide range of sources- to the atmosphere: by evaporation of water from the soil and water contained in the vegetation surface, on one hand, and by transpiration of the vegetation, on the other (Fig. 1). Evaporation is the physically based process of transferring water -stored in the soil or on the surface of canopies, stems, branches, soils and paved areas- to the atmosphere. Transpiration is the evaporation of water in the vascular system of plants through leaf stomata. The opening and closure of stomata is controlled by their guard cells. Hence, transpiration is a bio-physical process since it involves a living organism and its tissues (Verstraeten et al., 2008).

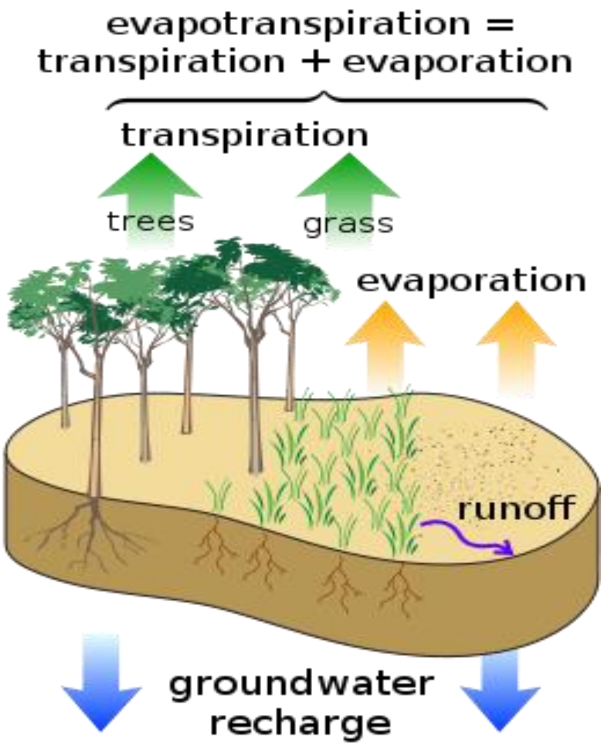

Figure 1. Evapotranspiration process.

The process of evapotranspiration is instrumental in temperature and water distribution in time and space (Eiseltová et al., 2012). Whilst evaporation is a passive process driven solely by solar energy input, transpiration involves an active movement of water through the body of plants transferring water from the soil to the atmosphere. The process of transpiration is also driven by solar energy but plants have the ability to control the rate of transpiration through their stomata and have developed many adaptations to conserve water when water is scarce. Evapotranspiration is an energy-driven process (Fig. 2). ET increases with temperature, solar radiation, and wind. On the other hand, ET decreases with increasing humidity.

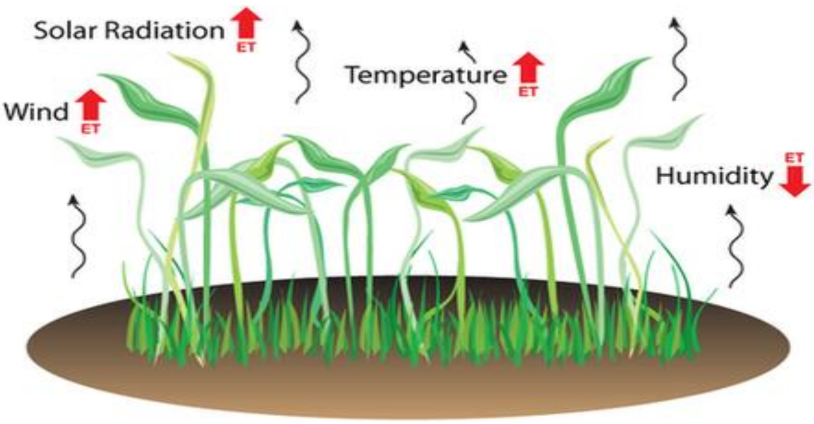

Figure 2. Weather variables that influence the ET process.

ET is one of the major elements of the hydrologic cycle, and its accurate prediction is of paramount importance for many investigations such as irrigation system design and management, hydrologic water balance, crop yield simulation, irrigation scheduling, drainage studies, agricultural and forest meteorology, and water resources planning and management (Kumar et al., 2002; Irmak et al., 2003; Chauhan & Shrivastava, 2009; Khoshravesh et al., 2017;

Liu et al., 2017). Actual crop evapotranspiration (ETc) are measurable using lysimeter, water balance approach, eddy covariance technique or imaging techniques, but their costs are very high (Kumar et al., 2002; Verstraeten et al., 2008; Valipour, 2015; Abdullah & Malek, 2016; Valipour, 2017). Therefore, field measurements of evapotranspiration are often spatially and temporally limited, and instead, ETc is usually calculated from estimated reference crop evapotranspiration (ETo) using the crop factor method, which consists of multiplying ETo with crop specific coefficients (kc) (Fig. 3) (Kumar et al., 2002; Yoder et al., 2005; Chauhan & Shrivastava, 2009; Khoshravesh et al., 2017). A more economical alternative for ETo estimation may be an indirect estimate based on climatological variables (Kumar et al., 2002; Landeras et al., 2008).

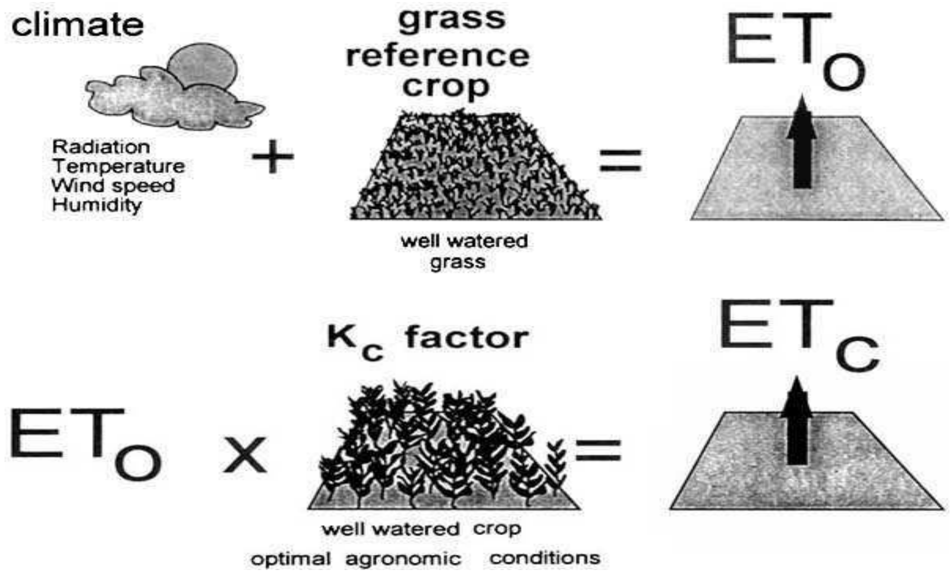

Figure 3. Calculation process of reference crop evapotranspiration (ETo), and actual crop evapotranspiration under standard conditions (ETc).

Over the past century, there has been a dramatic increase for the need to develop an accurate and standard method to estimate ETo (Jabloun & Sahli, 2008). The FAO 56 Penman-Monteith (FAO 56 P-M) equation, adopted by the international scientific community as the standard/reference method for determining ETo (Allen et al., 2006), has been ranked as the best method for all climatic conditions (Efthimiou et al., 2013). However, this method requires several climate measurements such as air temperature, relative humidity, solar radiation, and wind speed (Er-Raki et al., 2010). Meteorological stations that meet the requirement are very limited in many special ecosystems around the world. In high-mountain environments, such as the Andean páramo, meteorological monitoring is limited, and high-quality data is scarce (Córdova et al., 2015) due to the extreme weather conditions that prevent proper monitoring and frequent failure in establishing long-term measurement facilities. Herein, some authors researched the estimation of ETo using limited weather data (Todorovic et al., 2013; Córdova et al., 2015). In addition, ET studies are scarce in páramo sites being the most relevant researches carried out by Córdova et al. (2015) and Carrillo-Rojas et al. (2016).

To overcome the data scarcity issue, several alternative methodologies and equations have been proposed with less climate parameters for ETo estimation (Jabloun & Sahli, 2008; Er-Raki et al., 2010): It includes empirical equations (mass transfer-, radiation-, temperature-, and pan evaporation-based methods) (e.g. Tabari et al., 2013; Valipour, 2015; Valipour, 2017); regression models (Multiple linear, Bayesian, Robust and Multivariate Adaptive Regression Splines (MARS)) (e.g. González-Camacho et al., 2008; Kisi, 2016; Khoshravesh et al., 2017); and machine learning (artificial neuronal networks (ANN), random forests (RF) and support vector machine (SVM)) (e.g. Kumar et al., 2002; Trajkovic et al., 2003; Cervantes-Osornio et al., 2011; Kisi, 2013). Recently, a considerable number of literatures have grown up around the theme of calibration and comparison of the performance of different models and methods in different climates, assessing their performances with the FAO 56 P-M as the reference (Landeras et al., 2008; Er-Raki et al., 2010; Efthimiou et al., 2013; Shiri, 2017).

The main objective of this study is to compare and evaluate the performance of twenty-one empirical models, eight ANN models, and a MARS model in estimating daily reference evapotranspiration (ETo) compared to the FAO 56 P-M equation at the Andean páramo, where climate record is scarce. Firstly, we conducted a nonlinear, non-additive variable selection approach using a random forest to identify the most influential variables. Secondly, we assembled ANN models in different combinations of the variables in order of the variable importance according to the previous random forests analysis. Thirdly, we introduced an empirical equation for daily estimation of ETo applying MARS method under local climate conditions, using only solar radiation and relative humidity. The comparison would provide a practical guidance on the selection of the most appropriate ETo equation under super-humid conditions.

2. Material and methods

2.1 Study area

The meteorological data for this study came from two automatic weather stations, both located in the high-elevation páramo of Ecuador (Fig. 4).

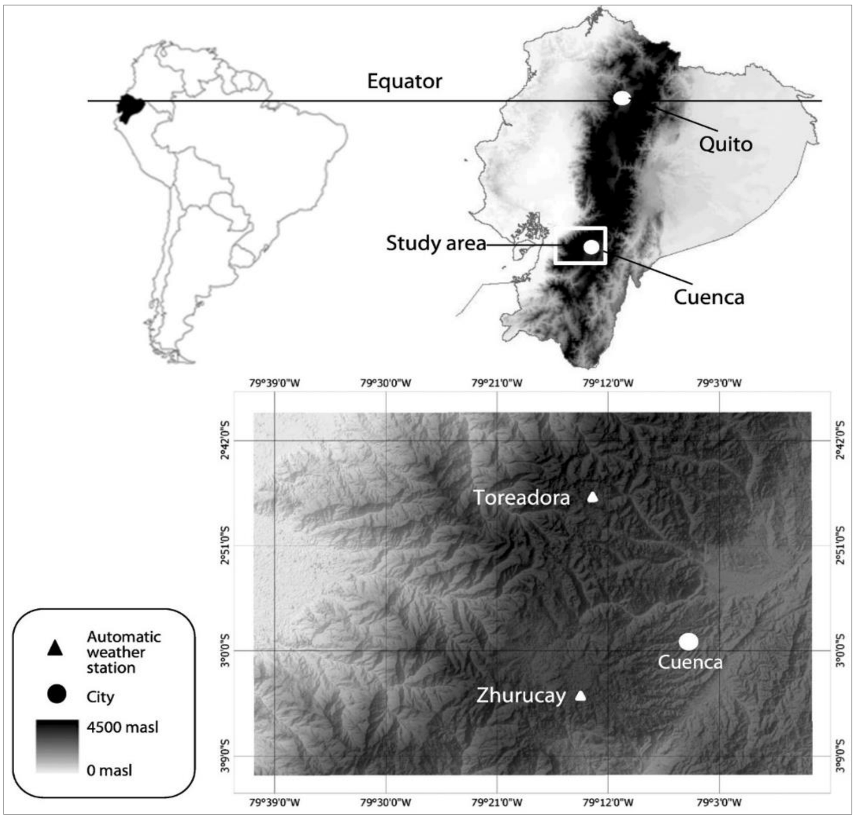

Figure 4. Locations of automatic weather stations.

- The Zhurucay weather station is situated in the Zhurucay catchment, affluent to the Jubones river basin (on the Pacific side of the Andes), draining to the Pacific Ocean, and situated 85 km south-west of Cuenca city (3°03′ S, 79°14′ W). The station is located at 3900 m a.s.l. with an average air temperature of 5.98 °C (maximum value 15.88 °C and minimum value -2.35 °C), average relative humidity of 91.44 %, solar radiation of 13.90 MJ m^{-1} day^{-1}, wind speed of 3.62 m s^{-1} and a precipitation of 1345 mm. One year of data were available (2014).

- The Toreadora weather station is located in the Quinuas catchment, in the headwaters of the Paute river basin (on the Atlantic side of the Andes), drains to the Amazon river, and situated 33 km of Cuenca city (2°47′ S, 79°13′ W). The station is located at 3955 m a.s.l. with an average climate values of: air temperature of 5.44 °C (maximum value 17.2 °C and minimum value -2.4 °C), relative humidity of 89.4 %, solar radiation of 12.13 MJ m^{-1} day^{-1}, wind speed of 2.31 m s^{-1} and a precipitation of 916 mm. Four years of data were available (2013 – 2016).

2.2 Methods for estimating reference evapotranspiration

The Penman-Monteith model incorporates thermodynamic and aerodynamic aspects with what has proven to be a very accurate method to estimate ETo anywhere (Allen et al., 2006). However, the greatest limitation for the use of this model is that it requires a large amount of meteorological data, limiting its use in places where these are not available. FAO 56 Penman-Monteith (FAO 56 P-M) model was used as reference for comparison and calibration of ETo equations. The form of the FAO 56 P-M equation is as follows:

$$ET_o = \frac{0.408 \cdot \Delta \cdot (R_n - G) + \gamma \cdot [900/(T + 273)] \cdot u \cdot (e_s - e_a)}{\Delta + \gamma \cdot (1 + 0.34 \cdot u)} \tag{1}$$

where

ET_o = reference evapotranspiration [mm day^{-1}],

R_n = net radiation at the crop surface [MJ m^{-2} day^{-1}],

G = soil heat flux density [MJ m^{-2} day^{-1}],

T = mean daily air temperature at 2 m height [°C],

u = wind speed at 2 m height [m s^{-1}],

e_s = saturation vapor pressure [kPa],

e_a = actual vapor pressure [kPa],

e_s-e_a = saturation vapor pressure deficit [kPa],

Δ = slope vapor pressure curve [kPa $°C^{-1}$],

γ psychrometric constant [kPa $°C^{-1}$].

The values of Δ, R_n, G, Y, e_s and e_a were calculated using the equations given by Allen et al. (2006) in the FAO irrigation and drainage study 56:

- **Slope vapor pressure curve (Δ):**

$$\Delta = \frac{4098 \cdot \left[0.6108 \cdot \exp\left(\frac{17.27 \cdot \mathrm{T}}{\mathrm{T} + 237.3}\right)\right]}{(\mathrm{T} + 237.3)^2} \tag{2}$$

- **Soil heat flux density (G):**

$$\mathrm{G}_{\mathrm{mes,i}} = 0.07(\mathrm{T}_{\mathrm{mes,i+1}} - \mathrm{T}_{\mathrm{mes,i-1}}) \tag{3}$$

$$\mathrm{G} = 0$$

where

$T_{mes,i-1}$: average air temperature in month i -1 [°C],

$T_{mes,i+1}$: average air temperature in month i +1 [°C].

- **Psychrometric constant (γ):**

$$\gamma = 0.665 \cdot 10^{-3}\mathrm{P} \tag{4}$$

where

P: atmospheric pressure [kPa].

- **Saturation vapor pressure (e_s):**

$$\mathrm{e}°(\mathrm{T}) = 0.6108 \cdot \exp\left[\frac{17.27 \cdot \mathrm{T}}{\mathrm{T} + 237.3}\right] \tag{5}$$

$$\mathrm{e_s} = \frac{\mathrm{e}°(\mathrm{T_{max}}) + \mathrm{e}°(\mathrm{T_{min}})}{2} \tag{6}$$

where

e°(T): vapor saturation pressure in air temperature [kPa].

- **Actual vapor pressure (e_a) derived from relative humidity data:**

$$\mathrm{e_a} = \frac{\mathrm{e}°(\mathrm{T_{min}})\frac{\mathrm{HR_{max}}}{100} + \mathrm{e}°(\mathrm{T_{max}})\frac{\mathrm{HR_{min}}}{100}}{2} \tag{7}$$

where

$e°(T_{min})$: vapor saturation pressure at the minimum air temperature [kPa],

$e°(T_{max})$: vapor saturation pressure at the maximum air temperature [kPa],

HR_{max}: maximum relative humidity [%],

HR_{min}: minimum relative humidity [%].

- **Extraterrestrial radiation for daily periods (R_a):**

$$R_a = \frac{24 \cdot 60}{\pi} G_{sc} d_r [\omega_s \sin(\varphi) \sin(\delta) + \cos(\varphi) \cos(\delta) \sin(\omega)] \tag{8}$$

where

R_a: extraterrestrial radiation [MJ m^{-2} dia^{-1}],

G_{sc}: solar constant = 0.082 MJ m^{-2} min^{-1},

d_r: inverse relative distance Earth-Sun,

ω_s: sunset hour angle [rad],

φ: latitude [rad],

δ: solar declination [rad].

$$[\text{radians}] = \left[\frac{\pi}{180}\right] [\text{decimaldegrees}] \tag{9}$$

$$d_r = 1 + 0.033 \cdot \cos\left(\frac{2\pi}{365} J\right) \tag{10}$$

$$\delta = 0.409 \cdot \sin\left(\frac{2\pi}{365} J - 1.39\right) \tag{11}$$

where J is the number of the day in the year between 1 (January 1) and 365 (December 31).

$$\omega_s = \frac{\pi}{2} - \arctan\left[\frac{-\tan(\varphi)\tan(\delta)}{X^{0.5}}\right] \tag{12}$$

where

$$X = 1 - [\tan(\varphi)]^2 [\tan(\delta)]^2 \tag{13}$$

$$\text{and } X = 0.00001 \text{ if } X \leq 0$$

- **Clear-sky solar radiation (R_{so}):**

$$R_{so} = (0.75 + 2 \cdot 10^{-5} \cdot z) \cdot R_a \quad (14)$$

where

R_{so}: clear-sky solar radiation [MJ m^{-2} dia^{-1}],

z: station elevation above sea level [m].

- **Net solar or net shortwave radiation (R_{ns}):**

$$R_{ns} = 0.77 \cdot R_s \quad (15)$$

where

R_{so}: net solar or net shortwave radiation [MJ m^{-2} dia^{-1}],

R_s: the incoming solar radiation [MJ m^{-2} day^{-1}].

- **Net longwave radiation (R_{nl}):**

$$R_{nl} = \sigma \left[\frac{T_{max,K}{}^4 + T_{min,K}{}^4}{2}\right] \left(0.34 - 0.14\sqrt{e_a}\right) \left(1.35 \frac{R_s}{R_{so}} - 0.35\right) \quad (16)$$

where

R_{nl}: net longwave radiation [MJ m^{-2} dia^{-1}],

σ: constant of Stefan-Boltzmann [4.903 x 10^{-9} MJ K^{-4} m^{-2} day^{-1}],

T_{max}, K: absolute maximum temperature during a 24-hour period [K = °C + 273.16],

T_{min}, K: absolute minimum temperature during a 24-hour period [K = °C + 273.16],

R_s/R_{so}: relative shortwave radiation (values ≤ 1.0).

- **Net radiation (R_n):**

$$R_n = R_{ns} - R_{nl} \quad (17)$$

Twenty-two empirical models and their associated equations for the estimation of reference evapotranspiration, are presented in Table 1. The calculation and procedures of all the required parameters for ETo estimation through the different empirical models can be thoroughly explored within the literature references. The equations presented in Table 1 were divided in four groups: temperature-based, radiation-based, combination-based and mass transfer-based.

Table 1. Selected models to estimate potential daily evapotranspiration with their reference, formula, and parameterization.

Model	Reference	Formula
Temperature-based		
Schendel (SCH)	Schendel (1967)	$ET_o = 16 \cdot \frac{T}{RH}$
Hargreaves–Samani (H-S)	Hargreaves & Samani (1985)	$ET_o = 0.0023 \cdot (T_{max} - T_{min})^{0.5} \cdot (T + 17.8) \cdot R_a$
Baier-Robertson (B-R)	Baier & Robertson (1965)	$ET_o = 0.157 \cdot T_{max} + 0.158(T_{max} - T_{min}) + 0.109 \cdot R_a - 5.39$
McCloud (MC)	McCloud (1955)	$ET_o = 0.254 \cdot 1.07^{1.8T}$
Radiation-based		
Jones-Ritchie (J-R)	Jones & Ritchie (1990)	$ET_o = \alpha \cdot (0.00387 \cdot R_s(0.6 \cdot T_{max} + 0.4 \cdot T_{min} + 29)$ $5°C < T_{max} < 35°C\ \alpha = 1.1$ $T_{max} > 35°C\ \alpha = 1.1 + 0.05 \cdot (T_{max} - 35)$ $T_{max} < 5°C\ \alpha = 0.1 \cdot \exp[0.18 \cdot (T_{max} + 35)]$
Irmak (IR)	Irmak et al. (2003)	$ET_o = -0.611 + 0.149 \cdot R_s + 0.079 \cdot T$
Makkink (MK)	Makkink (1957)	$ET_o = 0.61 \cdot \frac{\Delta}{\Delta + \gamma} \cdot \frac{R_s}{\lambda} - 0.12$
Turc (TR)	Turc (1961)	$ET_o = a_T 0.013 \cdot \frac{T}{T + 15} \cdot \frac{23.8856 \cdot R_s + 50}{\lambda}$ $RH \geq 50\%\ a_T = 1$ $RH < 50\%\ a_T = 1 + (50 - RH)/70$
Jensen-Haise (J-H)	Jensen & Haise (1963)	$ET_o = 0.0102 \cdot (T + 3) \cdot R_s$
Priestley-Taylor (P-T)	Priestley & Taylor (1972)	$ET_o = 1.26 \cdot \frac{\Delta}{\Delta + \gamma} \cdot \frac{R_n - G}{\lambda}$

Tabari (TB)	Tabari et al. (2013)	$ET_o = -0.642 + 0.174 \cdot R_s + 0.0353 \cdot T$
Copais (CP)	Alexandris et al. (2006)	$ET_o = 0.057 + 0.227 \cdot C_2 + 0.643 \cdot C_1 + 0.0124 \cdot C_1 \cdot C_2$ $C_1 = 0.6416 - 0.00784 \cdot RH + 0.372 \cdot R_s - 0.00264 \cdot RH \cdot R_s$ $C_2 = -0.0033 + 0.00812 \cdot T + 0.101 \cdot R_s + 0.00584 \cdot T \cdot R_s$
Combination-based		
Valiantzas (VT1)	Valiantzas (2013)	$ET_o = 0.051 \cdot (1-\alpha) \cdot R_s \cdot \sqrt{T+9.5} - 0.188 \cdot (T+13) \cdot \left(\frac{R_s}{R_a} - 0.194\right) \cdot \left[1 - 0.00015 \cdot (T+45)^2 \cdot \sqrt{RH/100}\right] - 0.0165 \cdot R_s \cdot u^{0.7} + 0.0585 \cdot (T+17) \cdot u^{0.75} \cdot \frac{[(1+0.00043 \cdot (T_{max} - T_{\min})^2)^2 - HR/100]}{[1+0.00043 \cdot (T_{max} - T_{\min})^2]} + 0.0001z$
Valiantzas (VT2)	Valiantzas (2013)	$ET_o = 0.00668 \cdot R_a \cdot \sqrt{(T+9.5) \cdot (T_{max} - T_{dew})} - 0.0696 \cdot (T_{max} - T_{dew}) - 0.024 \cdot (T+20) \cdot \left(1 - \frac{RH}{100}\right) - 0.0455 \cdot R_a \cdot (T_{max} - T_{\mathrm{dew}})^{0.5} + 0.0984 \cdot (T+17) \cdot [1.03 + 0.00055 \cdot (T_{max} - T_{\min})^2 - (RH/100)]$
Rijtema (RI)	Rijtema (1968)	$ET_o = \frac{\left(\frac{\Delta \cdot Rn}{\lambda}\right) + \gamma \cdot r \cdot u^{0.75} \cdot (e_s - e_a)}{(\Delta + \gamma)}$
Mass transfer-based		
Mahringer (MA)	Mahringer (1970)	$ET_o = 2.86 \cdot u^{0.5} \cdot (e_s - e_a)$
Trabert (TR)	Trabert (1896)	$ET_o = 3.075 \cdot u^{0.5} \cdot (e_s - e_a)$
WMO	WMO (1966)	$ET_o = (1.298 + 0.934 \cdot u) \cdot (e_s - e_a)$
Brockamp-Wenner (B-W)	Brockamp & Wenner (1963)	$ET_o = 5.43 \cdot u^{0.456} \cdot (e_s - e_a)$
Rohwer (RO)	Rohwer (1931)	$ET_o = (3.3 + 0.891 \cdot u) \cdot (e_s - e_a)$
Penman (PE)	Penman (1948)	$ET_o = (2.625 + 0.713 \cdot u) \cdot (e_s - e_a)$

ET_o is the reference crop evapotranspiration (mm day^{-1}), R_n is the net radiation (MJ m^{-2} day^{-1}), G is the soil heat flux (MJ m^{-2} day^{-1}), γ is the psychrometric constant (kPa/°C), λ is the latent heat of

vaporization (MJ kg^{-1}), e_s is the saturation vapor pressure (kPa), e_a is the actual vapor pressure (kPa), Δ is the slope of saturation vapor pressure-temperature curve (kPa/°C), T is the average daily air temperature (°C), u is the mean daily wind speed at 2 m (m/s), r is the roughness coefficient, z is the site elevation (m), T_{min} is the minimum air temperature (°C), T_{max} is the maximum air temperature (°C), T_{dew} is the dew point temperature (°C), RH is the average relative humidity (%), R_a is the extraterrestrial radiation (MJ m^{-2} day^{-1}), R_s is the solar radiation (MJ m^{-2} day^{-1}), and α is equal to 0.23. For calculation of T and T_{dew}, refer to Allen et al. (2006). To obtain roughness coefficient values (r) for the páramo ecosystem refer to Poulenard et al. (2001).

2.3 Validation and calibration of simplified methods

The models (Table 1) were validated and calibrated according to the recommendations from FAO Methodologies for Crop Water Requirements for new regions using ETo standard FAO 56 P-M definition (Irmak et al., 2003). To calibrate the empirical models against FAO 56 P-M, the calibration method described in Fooladmand & Haghighat (2007), Tabari & Talaee (2011) and Mehdizadeh et al. (2017) was used. The calibration radius (cr) was computed on a daily basis as:

$$cr = \frac{ET_o FAO56PM}{ET_o \text{Model}} \tag{18}$$

Calibration values on a daily basis were averaged into one main value. They were not chosen to work with monthly values due to the limited weather database (2013-2015 calibration period from Toreadora weather station). Thus, for validation 2016 period (Toreadora weather station) and 2014 period (Zhurucay weather station) were used. Zhurucay station is validated with the calibration of Toreadora station for two main reasons: 1) incomplete weather database for Zhurucay weather station and 2) both weather stations are located in the same geographical area, ecosystem type, and at similar elevations.

2.4 Variable importance measured with random forests

The procedure of random forests is a popular and efficient algorithm based on model aggregation concepts, and is applicable for classification and regression problems. It was proposed by Breiman (2001). The principle of random forests is to combine many binary decision trees built using several bootstrap samples coming from a learning sample (*L*) and choosing randomly at each node a subset of explanatory variables (*X*) (Genuer et al., 2010). More precisely, with respect to the well-known "classification and regression trees" (CART) model building strategy (Breiman et al., 1984) performing a growing step followed by a pruning one, two differences can be noted. First, at each node, a given number of input variables are randomly chosen and the best split calculated only within this subset. Second, no pruning step is performed so all the trees of the forests are maximal trees.

The quantification of the variable importance is an important issue in many applied problems complementing variable selection by interpretation issues (Genuer et al., 2010). In the random forests framework, the most widely used score of importance of a given variable is the increasing in mean of the error of a tree (mean square error (MSE) for regression and misclassification rate for classification) in the forest when the observed values of this variable are randomly permuted in the "out-of-bag" (OOB) samples (it could be slightly negative). Often, such random forests variable importance is called permutation importance indices the opposition to total decrease of node impurity measures already introduced in the seminal book about CART by Breiman et al. (1984). Random forests for determining variable importance has been widely studied (Sandri & Zuccolotto, 2006; Strobl et al., 2007; Strobl et al., 2008; Genuer et al., 2010; Hapfelmeier & Ulm, 2013).

At the same time, weather data input in FAO 56 P-M equation are variables obtained by direct measure (solar radiation, temperature, relative humidity, wind, and atmospheric pressure), and thus these were analyzed with random forests (Table 2). The *Salford Predictive Modeler 8* software was used for measuring variable importance through random forests tool.

Table 2. Variable importance of FAO 56 P-M equation inputs applying random forests.

Variable	Score
R_s	100
HR_{min}	46.84
T_{max}	19.94
HR_{max}	2.40
u	1.85
T_{min}	1.06
P	1.02

T_{max} (maximum air temperature in °C), T_{min} (minimum air temperature in °C), R_s (solar radiation in W/m^2), HR_{min} (minimum relative humidity in %), HR_{max} (maximum relative humidity in %), u (wind speed at 2 m height in m/s), P (atmosphere pressure in mbar).

2.5 Artificial neural networks

ANNs are considered a connecting computational tool that emulates the function of neural networks in biological systems (Landeras et al., 2008). ANNs extract the relationship of inputs and outputs of a process, without explicitly knowing the physical nature of the problem in such a way that the result is transmitted in the network until a signal output is given. The procedure of ANN-based models is, in general, divided into training, validation and testing performances (Abdullah & Malek, 2016). The architecture of an ANN has an input layer (where data are introduced to an ANN), the hidden layer(s) (where data are processed), and the output layer (where results of given inputs are provided). ANNs have been widely applied for estimating ETo as a function of climatic variables (Kumar et al., 2002; Trajkovic et al., 2003; González-Camacho et al., 2008; Chauhan & Shrivastava, 2009).

The ANNs models were applied using the software NeuralTools 7.5 (Palisade Corporation). The ANN type was the Multi-Layer Feedforward Network (MLFN) or Multi-Layer Perceptron Network. A sigmoidal function was used as activation in hidden layer neurons. Specifically, NeuralTools uses a hyperbolic tangent function. Training consists of finding a set of connection weights and bias terms that direct the network to generally the right answers. During the training process, the Conjugate Gradient Descent method, together with the Simulated Annealing method, were used according to Bishop (1995) and Masters (1995). To avoid over-learning of ANNs models, the available training data (2013-2015; Toreadora weather station) were divided in two subsets: 80 % of patterns for training and 20 % for cross validation. The 2016 period for the Toreadora weather station and for the 2014 period of the Zhurucay weather station were used for independent validations of the models. According to Koleyni (2010), the performance of a neural network is very often related to its architecture. This performance is usually determined through test-error experiments due to lack of theory (Laaboudi et al., 2012). In order to avoid this time consuming task, NeuralTools software allows one to choose the option “Best Net search” to obtain the best neural network configuration and architecture across test-error performance. The advantage of the neural method relies on the possibility of improving performance criteria by modifying network architecture (Laaboudi et al., 2012).

The combination of inputs (daily values of weather parameters) for each ANN was selected after variable selection with random forests (Table 2). The three most important parameters were solar radiation, minimum relative humidity, and maximum air temperature. The inputs of ANNs were chosen in order to implement models that use the least number of weather variables. A summary of inputs is given in Table 3.

Table 3. Inputs for the application of each ANN.

Variable inputs	ANN1	ANN2	ANN3	ANN4	ANN5	ANN6	ANN7	ANN8
R_s	•	•	•	•	•	•	•	
HR_{min}	•	•	•	•	•	•		•
T_{max}	•	•	•	•	•		•	•
HR_{max}	•	•	•	•				
u	•	•	•					
T_{min}	•	•						
P	•							

Units are the same as in Table 2.

2.6 Multivariate adaptive regression splines (MARS)

MARS is a non-parametric model of non-linear regression that allows explaining the dependence of the response variable on one or more explanatory variables (Fridedman, 1991). Non-parametric modeling does not approximate one single domain-wide function, but adjusts it to several other functions for simple metrics, usually low-order polynomials, defined on a sub-region of the domain (parametric adjustment per section), or sets a simple function for each value of the variable (global setting) (Sánchez-Molina & Poveda-Jaramillo, 2006). MARS is usually preferred because it allows one to approximate complex nonlinear relationships from data, without postulating a hypothesis about the type of non-linearity present. For example, the construction of the algorithm model incorporates mechanisms that allow selection of relevant explanatory variables. Also, the resulting model is easier to interpret as opposed to black box models such as artificial neural networks; finally, the estimation of its parameters is computationally efficient and rapid (Velásquez-Henao et al., 2014). In Friedman (1991), MARS algorithm is fully presented with aspects related to non-metric modeling and adaptive computing. The *Salford Predictive Modeler 8* software was used for obtained the MARS regression. MARS method has been widely used for non-linear time series forecasting (e.g. Sánchez-Molina & Poveda-Jaramillo, 2006; Velásquez-Henao et al., 2014).

MARS was applied for weather inputs in the FAO 56 P-M equation. Local páramo conditions were analyzed by a non-parametric regression, and this is the model that this research proposes as the Reference Evapotranspiration Model for Páramo Ecosystems now called REMPE equation. Data from the Toreadora weather station (2013-2015 period), were used for the regression analysis. Additionally, data from the periods 2016 (Toreadora) and 2014 (Zhurucay) were used for independent validation analysis of the equation.

The REMPE equation is shown below (R_s is in W/m^2, and HR_{min} is in %):

```
BF1 = max( 0, Rs - 151.949);
BF2 = max( 0, 151.949 - Rs);
BF3 = max( 0, RHmin - 82.5);
BF4 = max( 0, 82.5 - RHmin);
BF5 = max( 0, Rs - 234.782);
BF6 = max( 0, Rs - 114.839).

REMPE ETo= 1.77954 + 0.0064776 * BF1 - 0.00793659 * BF2 - 0.0256779 * BF3
             + 0.0188508 * BF4 - 0.00135548 * BF5 + 0.001299 * BF6
```

2.7 Model comparison analysis

To analyze similarities and differences among models, the following parameters were employed: 1) mean bias error (MBE): is a measure that indicates the average tendency of the simulated data to be greater or smaller than the observed data, i.e. to reflect the systematic of a model to overestimate or underestimate values, 2) mean absolute error (MAE): measures the average magnitude of the errors in a set of predictions, without considering their direction. It's the average over the test sample of the absolute differences between prediction and actual observation where all individual differences have equal weight, and 3) root mean square error (RMSE): is a quadratic scoring rule that measures the average magnitude of the error. It's the square root of the average of squared differences between prediction and actual observation, this metric is sensitive to peaks.

$$\boldsymbol{MBE} = \frac{1}{\boldsymbol{n}}\sum_{\boldsymbol{i}=1}^{\boldsymbol{n}}(\boldsymbol{P_i} - \boldsymbol{O_i}) \tag{19}$$

$$\boldsymbol{MAE} = \frac{1}{\boldsymbol{n}}\sum_{\boldsymbol{i}=1}^{\boldsymbol{n}}|\boldsymbol{P_i} - \boldsymbol{O_i}| \tag{20}$$

$$\boldsymbol{RMSE} = \sqrt{\frac{1}{\boldsymbol{n}}\sum_{\boldsymbol{i}=1}^{\boldsymbol{n}}(\boldsymbol{P_i} - \boldsymbol{O_i})^2} \tag{21}$$

where:

Oi = observed value; Pi = simulated value; n = considered data.

3. Results and Discussion

3.1 Analyses of influential weather variables and model performance

Random forest results, the assembly of artificial neural networks models and MARS method equation were establish in the previous sections. According to the Random forest analysis, the dominant variable influencing the ETo estimate was solar radiation (Table 2). The importance level of solar radiation was also found by Córdova et al. (2015) and it is referred to as a key factor in the FAO 56 P-M equation for ETo estimation in páramo ecosystems. The second dominant variable was minimum relative humidity, which is explained by a recognized weather pattern in wet ecosystems, thus high relative humidity reduces the total evapotranspiration rate, and on the contrary, evapotranspiration increases when humidity decrease (Gong et al., 2006). Minimum relative humidity would have stronger influence on maximum relative humidity because of its higher intradaily variation (Fig. 5).

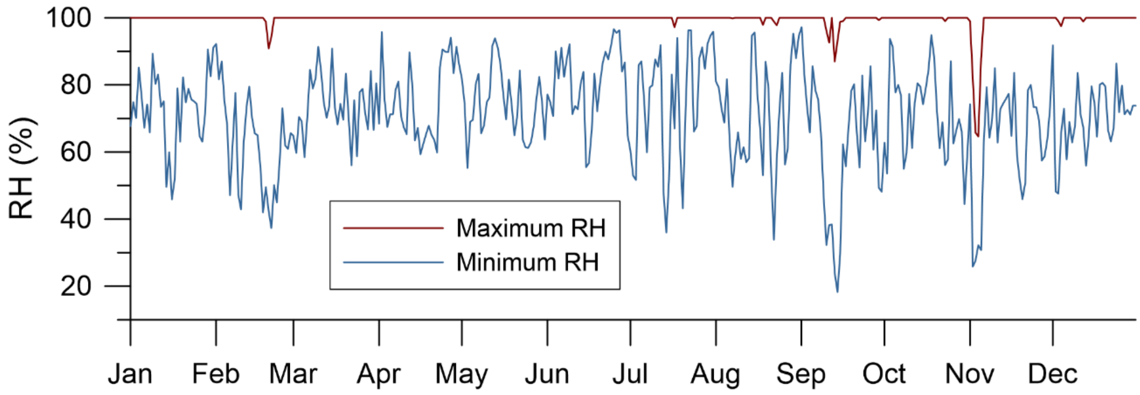

Figure 5. Example of maximum and minimum relative humidity pattern (2015 period of Toreadora weather station).

Results from the random forest analysis also revealed that the least dominant variables for ETo estimation were wind and atmospheric pressure. This is corroborate by Córdova et al. (2015) who determine that wind is the least important variable for ETo estimation in this environment. Eight ANN models were assembled to use the minimum number of input variables (Table 3), while the MARS method helped obtain REMPE, which incorporated solar radiation and minimum relative humidity as the dominant input variables. The results showed that the variable discrimination procedure performed by MARS is in conformity with the variable order of importance classified by the random forest procedure.

3.2 Comparison of methodologies for ETo estimation

This section will focus specifically on the statistical comparison of the different methodologies for ETo estimation. For both weather stations, the total performance of different groups of ETo equations in the original form are presented in Figure 6, whilst in Figure 7 is presented the comparison of the calibrated form of ETO equations. Simple statistical metrics (MBE, MAE and RMSE) were used in order to evaluate the overall performance of the models against to the FAO 56 P-M model. The numerical values obtained through the statistical metrics are presented in Appendix 10 and 11.

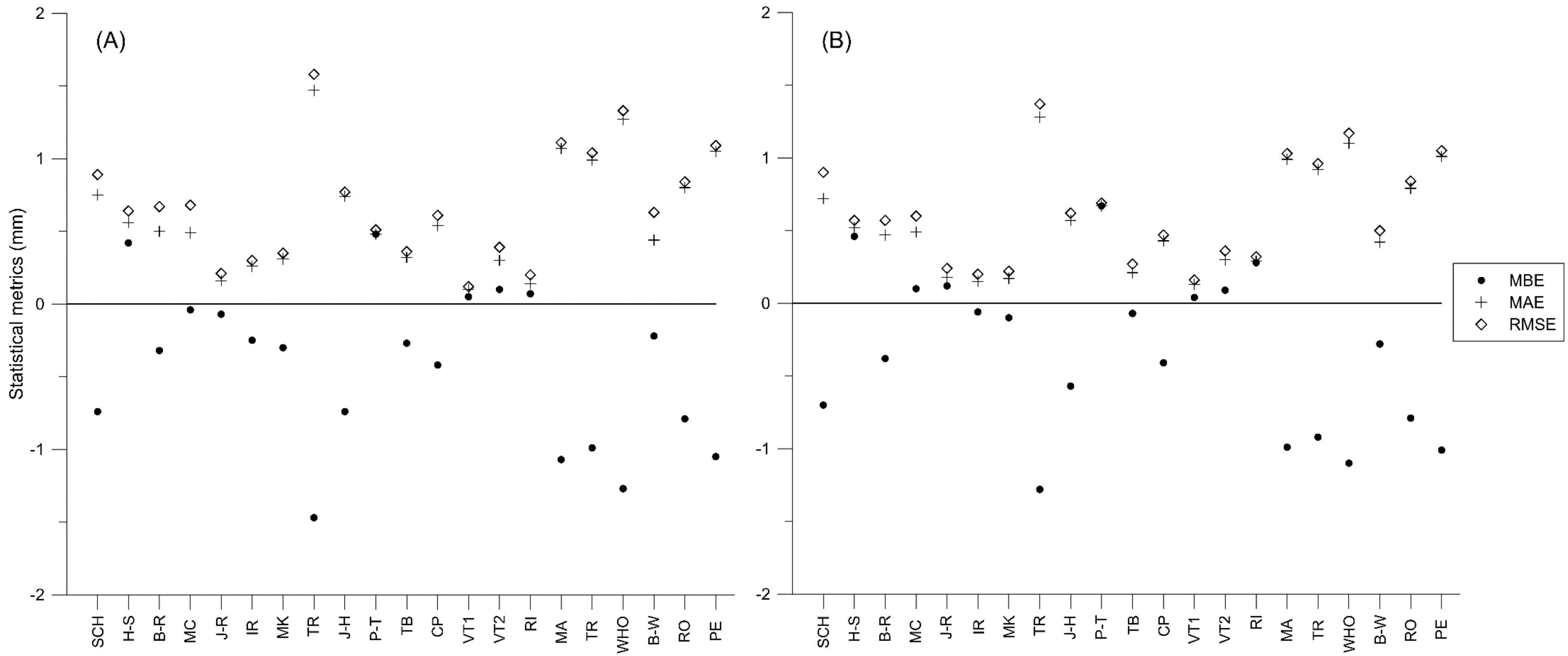

Figure 6. Graphical representation of statistical performance of the different ETo estimation methods versus FAO 56 P-M model. A) Toreadora weather station; B) Zhurucay weather station.

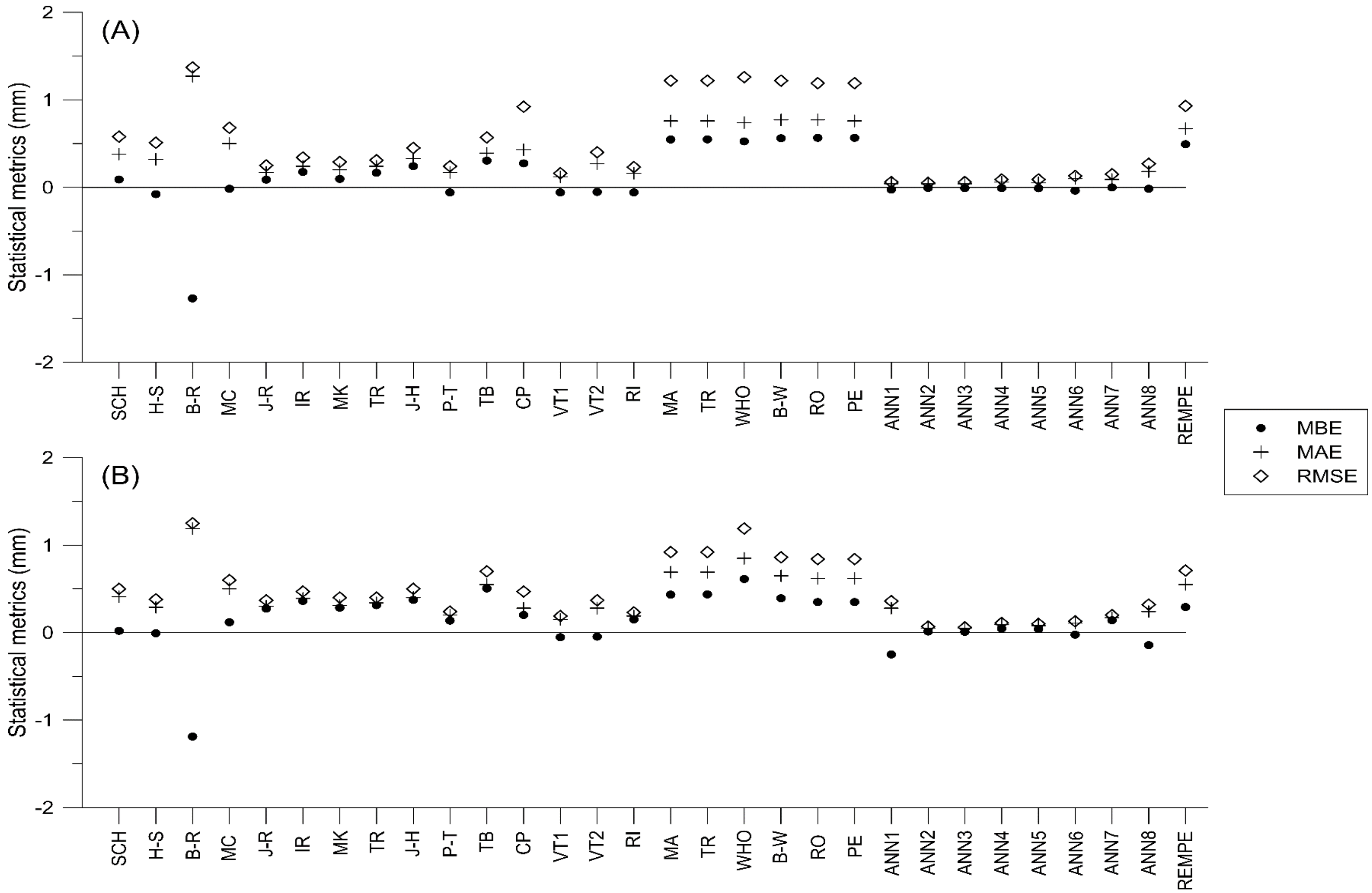

Figure 7. Graphical representation of statistical performance of the different calibrated ETo estimation methods versus FAO 56 P-M model. A) Toreadora weather station; B) Zhurucay weather station.

3.2.1 Empirical models

Result comparison of the empirical equations, showed that the combination-based grouping method presented the best estimation for model fitting with the lowest statistical values. The second best method corresponded to the radiation-based grouping, followed by the temperature-based. The mass transfer-based grouping showed the worst estimate for model fitting. The same tendency was found by Liu et al. (2017) despite being investigated in a different environment. This is explained by the fact that the combination-based equations incorporate all, or most, of the weather variables and result in better performances. In terms of precision, VT1 was a better equation with regard to the combination-based grouping method in both weather stations. In fact, VT1 and VT2 equations derive from FAO 56 P-M model (Valiantzas, 2013), and thus indicate a high level of performance. However, while the VT1 equation incorporates whole data sets, the VT2 equation does not require wind speed data. In spite of this, the VT2 performance was excellent. This demonstrates that wind speed is a not a powerful variable. In addition, the RI equation needs a precise roughness value to obtain high performance, for which the roughness values provided by Poulenard et al. (2001) for three páramo sites were used.

Results from the radiation-based grouping method also showed high performance. J-R was the best model for data from the Toreadora weather station, followed by IR, TB and MK; whereas for data from the Zhurucay weather station, IR was the best model, followed by MK, J-R and TB. This might be explained by the stronger influence of the solar radiation variable on ETo estimation after random forest analysis. Lu et al. (2005) and Xu & Singh (2002) have suggested that radiation-based approaches performed better than temperature-based approaches, all of which corroborate the findings in this study. J-H, P-T and CP models revealed moderate performance, whereas TR model showed the poorest performance for both weather stations. In the case of TR model, results in this study contradict those from Trajkovic & Kolakovic (2009) which indicate that the Turc equation is suited for ETo estimations in humid areas.

The results from the temperature-based grouping method were very similar to those from the radiation-based grouping method, which showed models with regular and high performances. Maximum and minimum temperature variables have an acceptable power to explain ETo estimate after the random forest analysis. For both weather stations MC was the best model; B-R and H-S were intermediate and SCH was the poorest. According to Almorox et al. (2015), temperature-based models in tropical climates might involve important variations depending upon fluctuations of specific local weather, where temperature alone might not be enough for proper estimations of ETo. In this study, most of the temperature-based models did not take into account solar radiation, vapor pressure deficit, or sunlight duration, corroborating the above statement. The mass transfer-based grouping method presented the poorest performance. This result may be explained by the fact that the hygrometric deficit (e_s-e_a) is very small in páramo areas, and so it may not have a significant effect for ETo estimation. Also, the incorporated wind speed variable in the equations might have had a negative effect on this method’s performance, as it was show by the random forest analysis (see above paragraphs). Singh & Xu (1997) and Gong et al. (2006), also mentioned that wind speed is not a significant factor for ETo estimation models. Valipour (2017) stated that estimating precision of mass transfer-based models is sensitive to parameter variation in each model. The B-R model showed to be an acceptable estimation model for both stations in the mass transfer-based grouping method. No other model provided good estimates. Similar results were found by Tabari et al. (2013), they showed that the mass transfer-based equations had the worst performances, while the radiation-based and temperature-based models were the best-suited equations for ETo estimate.

3.2.2 Calibration of empirical models

Depending upon the equation used, the values obtained after comparing the original and calibrated models, showed several differences (Figure 6 and 7). Models with a cr value close to 1 denote that the estimated values compared to the values derived from the original equation almost equal those obtained with the FAO 56 P-M equation (MC, J-R, VT1, VT2 and RI). After calibration (cr ≈ 1), models that showed the best performances were not expected to improve significantly. Comparison of temporal estimations of reference evapotranspiration per group for 21 empirical models in their original and calibrated form are shown in Appendix 1 to 6**.** The different corresponding groups with regard to the FAO 56 P-M model are shown for validation periods with data from the Toreadora (2016) and Zhurucay (2014) weather stations. Generally, ETo equations should improve performance after calibration. Surprisingly, this is observed for about half of the models. With data from the Toreadora weather station, SCH, H-S, IR, CP, MK, J-H and P-T models showed an increased performance and from Zhurucay weather station SCH, H-S, J-H, P-T and CP models showed an increased performance. For both weather stations, the TR model increased its performance considerably following calibration. No significant improvement was observed for the remaining models.

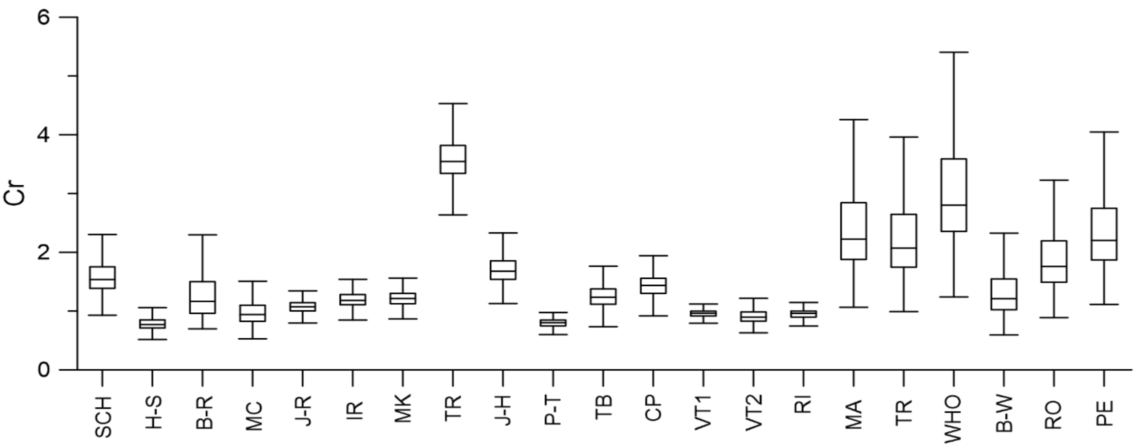

Figure 8. Box plot of calibration radiuses (cr) for 21 empirical models. The median (center line), interquartile range (25% to 75%) (box) and interquartile range (0-25% and 75-100%) multiple to a factor (1.5) (whiskers).

The results obtained after calibration for temperature-based grouping is in agreement with the recommendation by Bautista et al. (2009) that temperature-based models should not be used without a preliminary local calibration in a tropical sub-humid climate. The calibration process is also recommended for the radiation-based grouping models, for example, Sentelhas et al. (2010) concludes that the application of the P-T model is recommended only after a local calibration. All mass transfer-based models, with the exception of B-W, improved their performance after calibration, but these are still poor estimating methods. It can be observed in Appendix 5 and 6, that all models of this group greatly overestimate the high peak ETo values, after calibration. In contrast, some models present better performances in the original uncalibrated form compared to the calibrate form (B-R, TB, IR and B-W). Such unpredictability could be explained by the high variability in the distribution of cr values. This is easily observed within box plots (Fig. 8), and suggest that this calibration method may not be the most precise one for model performance improvement. Despite this, several of the models with low cr value variability improved their performances to acceptable results.

Estimation accuracy during calibration and validation periods indicated suitability of the combination-based, radiation-based and temperature-based models for ETo simulations in the páramo ecosystem. Based on the statistics, results determined that mass transfer-based models are not accurate for the estimation of ETo in páramo ecosystems.

3.2.3 Artificial neural networks models

All ANNs models showed high performances for data from both weather stations surpassing all empirical models to a large extent. From ANNs models, ANN2 was the best model for Toreadora, and ANN3 for Zhurucay, weather stations. Comparison of temporal estimations of reference evapotranspiration for the 8 ANNs models in the corresponding validation period for Toreadora weather station are show in Appendix 7 and for Zhurucay in Appendix 8. The ANNs models for the Toreadora weather station proved less error than that of the Zhurucay weather station because its calibration was done with data from the Toreadora weather station. Despite, the ANN models were calibrated with Toreadora weather station database, the models adjusted very well to the validation period of Zhurucay weather station. Better results could have been obtained if there were complete climate databases for the Zhurucay weather station.

ANN1 model for Zhurucay weather station is the less accurate for ETo estimation due to the atmospheric pressure variable that probably introduced noise in the ANN model disturbing its performance. ANN6 to ANN8 models were assembled in different combinations of two or three main climate parameters to avoid risks of sensor failure. The ANN8 model did not incorporate solar radiation variable, and consequently its performance was low compared to the other models. In spite of that, this model revealed to be much better than any of the empirical models used for ETo estimations. The “Best Net search” option facilitated the determination of the structure configuration for each ANN model. This option allowed to obtain satisfactory results (Table 4). Results from the prediction accuracy analysis suggested ANNs as a powerful tool for modeling ETo in super-humid conditions. This is corroborated by several ETo estimation studies that highlighted the high accuracy of ANNs in relation to other methods (e.g. Abdullah & Malek, 2016).

Table 4. Summary of training and cross validation processes of the evaluated ANNs.

Model	Type	Structure	RMSE Training (mm day^{-1})	RMSE Testing (mm day^{-1})	Inputs
ANN1	MLFN	7-5-1	0.048	0.046	R_s, $HR_{min,max}$, $T_{min,max}$, u, P
ANN2	MLFN	6-3-1	0.051	0.056	R_s, $HR_{min,max}$, $T_{min,max}$, u
ANN3	MLFN	5-5-1	0.054	0.049	R_s, $HR_{min,max}$, T_{max}, u
ANN4	MLFN	4-5-1	0.062	0.064	R_s, $HR_{min,max}$, T_{max}
ANN5	MLFN	3-4-1	0.065	0.083	R_s, HR_{min}, T_{max}
ANN6	MLFN	2-3-1	0.104	0.104	R_s, HR_{min}
ANN7	MLFN	2-4-1	0.094	0.146	R_s, T_{max}
ANN8	MLFN	2-3-1	0.221	0.202	HR_{min}, T_{max}

Structure: number of inputs-number of neurons/nodes in the hidden layer-number of outputs.

3.2.4 MARS model

The REMPE equation showed an unexpected poor performance for both weather stations (RMSE = 0.93 and 0.71 in Toreadora and Zhurucay respectively). The equation overestimated daily ETo (MBE = 0.49 and 0.29 in Toreadora and Zhurucay respectively). Despite the fact that the equation was calibrated with data from the Toreadora weather station, it surprisingly performed better with data from the Zhurucay weather station. For both stations, REMPE model results surpassed those from mass transfer-based grouping method with the exception of the B-W model which presented better performance in its original form. Nevertheless, REMPE had a better performance in comparison to SCH, J-H and TR for Toreadora and SCH, H-S, B-R, TR, J-H, P-T and CP for Zhurucay, with all the models in their original form. On the other hand, REMPE performed better than B-R only, in Toreadora, and better than IR, B-R, TR, J-H and TB, in Zhurucay, after the calibration process for the rest of groupings. Comparison of temporal estimations of reference evapotranspiration for REMPE model in the corresponding validation period for each weather station, are show in Appendix 9.

REMPE produced a higher error with respect to the best results between the original and calibrated empirical models. Mass transfer-base models were the only exceptions. These findings were unexpected and represent the enormous number of factors involved in climate control, even at specific locations. This sensitivity makes it difficult to actually show that a simple equation, especially a non-linear one, can produce accurate predictions (Traore et al., 2010). The short time series of data used for the equation calibration, might have also limited its performance. In addition, the results obtained in this study are contradictory to the Aghajanloo et al. (2013) findings, in which their results showed that multiple non-linear regression (MNLR) models can be an acceptable approach to predict daily ETo. Aghajanloo et al. (2013) revealed that increasing the numbers of input variables into the MNLR models can improve the accuracy of ETo estimates.

3.2.5 Annual reference evapotranspiration

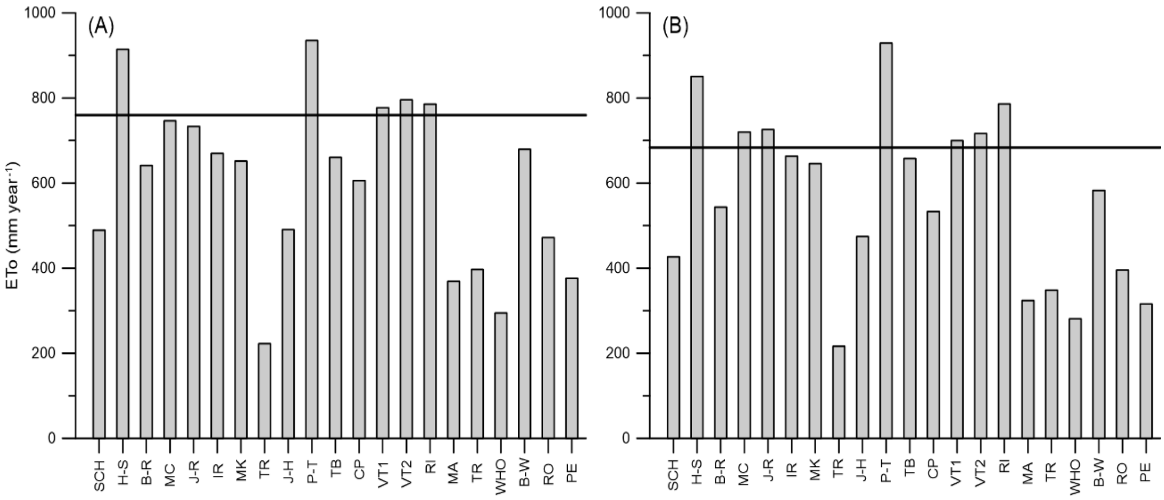

Figure 9. Annual ETo estimated from original empirical models. Solid line represents the reference model. A) data from Toreadora weather station; B) data from Zhurucay weather station.

Annual ETo was obtained from the sum of the daily ETo. The different ETo models to estimate annual ETo varied considerably. In regard to the original empirical equations, the combination-based grouping, MC and J-R models agreed very closely to the FAO 56 P-M ETo annual value in the case of data from Toreadora weather station (Fig. 9A). As for Zhurucay weather station data, models with the best adjustments were VT1, VT2, MK, J-R, IR and TB (Fig. 9B). The other models underestimated ETo compared with the FAO 56 P-M equation, and a few overestimated it for super-humid environments.

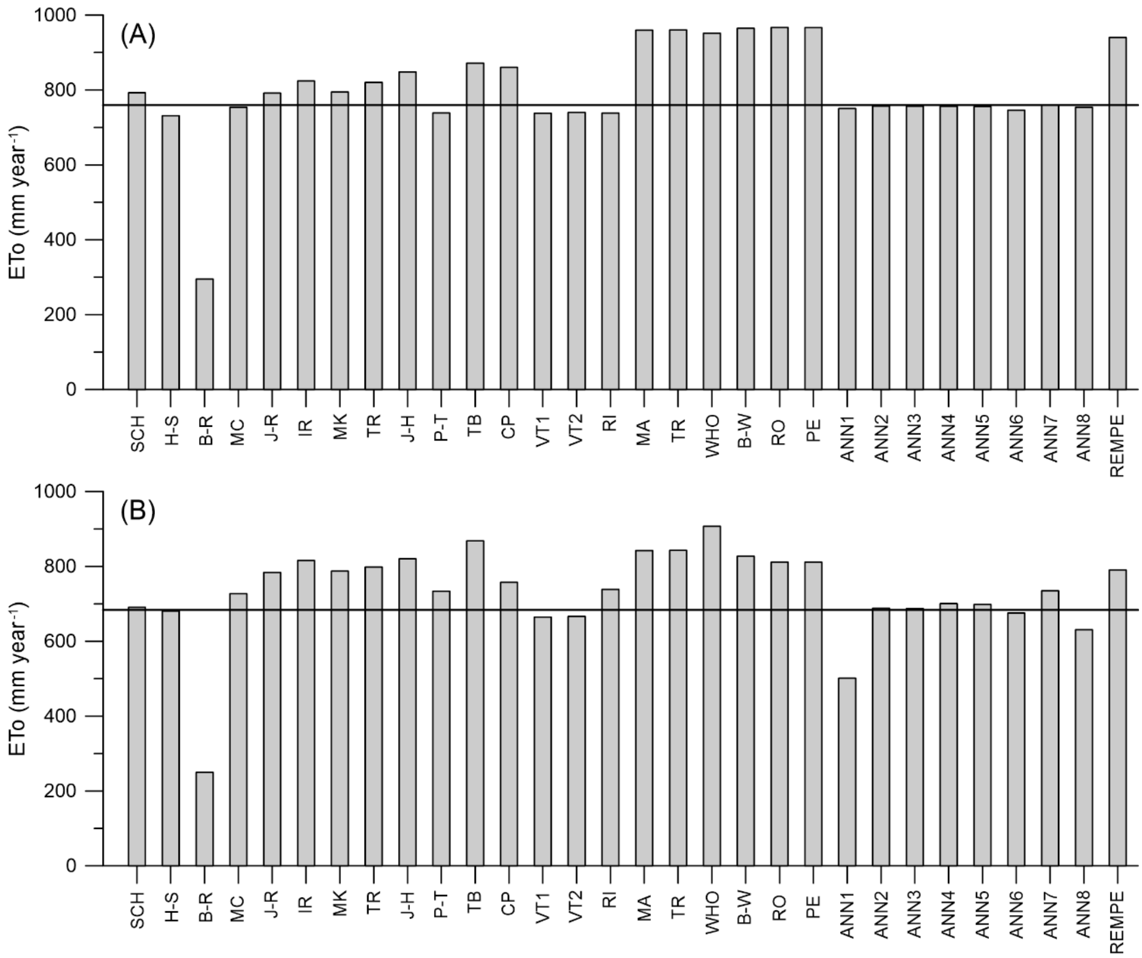

Figure 10. Annual ETo estimated from different calibrated methods. Solid line represents the reference model. A) data from Toreadora weather station; B) data from Zhurucay weather station.

Once the calibration procedure was applied, several models improved performance to estimate daily ETo. As a consequence, annual estimations improved as well. This can be clearly observed in Figure 10 for data from both weather stations. The radiation-based models were probably the ones that improved the most with respect to the other, especially for data from Toreadora weather station (Fig. 10A). ANNs models fit well with adjustments for data from both weather stations. Exemptions were ANN1 and ANN8 models for data from the Zhurucay weather station (Fig. 10B). The mass transfer-based models overestimated annual ETo values for data from both stations (Fig. 10). As opposed to the pattern described in the previous paragraph, once the calibration procedure was applied, most of the models overestimated ETo and only a few underestimated ETo compared to the FAO 56 P-M equation.

4. Conclusions

Prediction models that require a smaller number of weather parameters for ETo estimations are recommended in cases where complete weather data records are lacking or unavailable. Complete data sets are often absent for high mountain areas such as páramo ecosystems. The páramo ecosystem is considered a super-humid region, although no previous studies have been conducted to estimate ETo by means of comparison among different estimation methodologies. In this study, to estimate the ETo in páramo regions, the reference evapotranspiration model for páramo ecosystems (REMPE) was developed under local conditions. The REMPE equation was generated thought the method of multivariate adaptive regression splines (MARS). REMPE, 21 empirical equations, and eight artificial neural networks (ANNs) models were compared to the standard FAO 56 P-M model. Altogether, the combination-based models performed well, followed by the radiation-based and temperature-based models. The mass transfer-based models had poor performances, with the exception of B-W; however, results indicate that these later models are not recommended for ETo estimate in páramo regions because of the super-humid environmental conditions. The calibration method significantly improved the performances of several of the models used. Such an improving effect should be further explored in order to develop more advanced calibration methods.

ANN models were accurate in estimating ETo, although specific patterns observed are difficult to explain due to complex non-linear phenomena. Nevertheless, the fact that ANNs models include different combinations of weather variables so as to use the smallest possible number of inputs, without decreasing modeling performance, these models should be applied in first instances when estimating ETo in páramo ecosystems.

By developing REMPE, solar radiation and minimum relative humidity were incorporated into the model as required variables. However, the REMPE equation showed an unsatisfactory performance when compared to that of other empirical equations. Can adding more input variables to the REMPE equation result in an improvement in its performance? This is an open question for further research.

In terms of software, NeuralTools v7.5 and Salford Predictive Modeler v8 are user friendly for easy implementation of methods, so these are highly recommended for data modeling in similar studies.

The FAO 56 P-M equation served as a reference model in the absence of lysimeter measurements. At the same time, lysimeter measurements perform better than the FAO 56 P-M, or other costly methods. That being said, this study raises the question about whether or not FAO 56 P-M is a valid reference to be used under super-humid conditions. Additionally, lysimeter measurements are not yet available. Therefore, this research suggests that for future studies it is necessary to undertake lysimeter measurements and to assess differences between these two methods in very wet páramo regions.

Therefore, the results presented in this thesis show, on one hand, how to select an appropriate ETo equation to be applied in water-logged environments, and with limited climatic data. On the other hand, these results allow the use of simple and accurate methods for ETo estimate in a difficult mountain highland topography; often with scant resource availability assigned to weather monitoring.

It is proposed to continue the research line by applying other techniques of ET estimation (e.g. lysimeters and eddy covariance). In addition, it is recommended to include a greater number of meteorological stations spatially distributed in páramo locations, incorporate longer available time series of climatic data, and develop new empirical equations for páramo environments by applying different regression techniques (e.g. wavelet regression -WR-).

5. References

Abdullah, S. S., & Malek, M. A. (2016). Empirical Penman-Monteith equation and artificial intelligence techniques in predicting reference evapotranspiration: a review. *International Journal of Water*, *10*(1), 55-66.

Aghajanloo, M. B., Sabziparvar, A. A., & Talaee, P. H. (2013). Artificial neural network–genetic algorithm for estimation of crop evapotranspiration in a semi-arid region of Iran. *Neural Computing and Applications, 23*(5), 1387-1393.

Alexandris, S., Kerkides, P., & Liakatas, A. (2006). Daily reference evapotranspiration estimates by the “Copais” approach. *Agricultural Water Management, 82*(3), 371-386.

Allen, R. G., Pruitt, W. O., Wright, J. L., Howell, T. A., Ventura, F., Snyder, R., Itenfisu, D., Steduto, P., Berengena, J., Baselga, J., Smith, M., Pereira, L. S., Raes, D., Perrier, A., Alves, I., Walter, I., Elliott, R., & Smith, M. (2006). A recommendation on standardized surface resistance for hourly calculation of reference ET o by the FAO56 Penman-Monteith method. *Agricultural Water Management*, *81*(1), 1-22.

Almorox, J., Quej, V. H., & Martí, P. (2015). Global performance ranking of temperature-based approaches for evapotranspiration estimation considering Köppen climate classes. *Journal of Hydrology, 528*, 514-522.

Baier, W., & Robertson, G. W. (1965). Estimation of latent evaporation from simple weather observations. *Canadian journal of plant science*, *45*(3), 276-284.

Bautista, F., Bautista, D., & Delgado-Carranza, C. (2009). Calibration of the equations of Hargreaves and Thornthwaite to estimate the potential evapotranspiration in semi-arid and sub-humid tropical climates for regional applications. *Atmósfera, 22*(4), 331-348.

Bishop, C. M. (1995). *Neural networks for pattern recognition*. Oxford University Press.

Breiman, L. (2001). Random forests. *Machine learning, 45*(1), 5-32.

Brockamp, B., Wenner, H. (1963). Verdunstungsmessungen auf den Steiner See bei Münster. Dt Gewässerkundl Mitt, 7, 149-154.

Buytaert, W., Célleri, R., De Bièvre, B., Cisneros, F., Wyseure, G., Deckers, J., & Hofstede, R. (2006). Human impact on the hydrology of the Andean páramos. *Earth-Science Reviews*, *79*(1), 53-72.

Carrillo-Rojas, G., Silva, B., Córdova, M., Célleri, R., & Bendix, J. (2016). Dynamic mapping of evapotranspiration using an energy balance-based model over an Andean Páramo Catchment of Southern Ecuador. *Remote Sensing, 8*(2), 160.

Célleri, R., & Feyen, J. (2009). The hydrology of tropical Andean ecosystems: importance, knowledge status, and perspectives. *Mountain Research and Development*, *29*(4), 350-355.

Cervantes-Osornio, R., Arteaga-Ramírez, R., Vázquez-Peña, M. A., & Quevedo-Nolasco, A. (2011). Redes neuronales artificiales en la estimación de la evapotranspiración de referencia. *Revista mexicana de ciencias agrícolas, 2*(3), 433-447.

Chauhan, S., & Shrivastava, R. K. (2009). Performance evaluation of reference evapotranspiration estimation using climate based methods and artificial neural networks. *Water resources management*, *23*(5), 825-837.

Córdova, M., Carrillo-Rojas, G., Crespo, P., Wilcox, B., & Célleri, R. (2015). Evaluation of the Penman-Monteith (FAO 56 PM) method for calculating reference evapotranspiration using limited data. *Mountain Research and Development*, *35*(3), 230-239.

Dinerstein, E., Olson, D., Graham, D., Webster, A., Primm, S., Bookbinder, M., Ledec, G. (1995). A conservation assessment of the terrestrial ecoregions of Latin America and the Caribbean. The World Bank, Washington, D.C.

Efthimiou, N., Alexandris, S., Karavitis, C., & Mamassis, N. (2013). Comparative analysis of reference evapotranspiration estimation between various methods and the FAO56 Penman-Monteith procedure. *European Water*, *42*, 19-34.

Eiseltová, M., Pokorný, J., Hesslerová, P., & Ripl, W. (2012). Evapotranspiration–A driving force in landscape sustainability. *In Evapotranspiration-Remote Sensing and Modeling*. InTech.

Er-Raki, S., Chehbouni, A., Khabba, S., Simonneaux, V., Jarlan, L., Ouldbba, A., Rodriguez, J. S., & Allen, R. (2010). Assessment of reference evapotranspiration methods in semi-arid regions: Can weather forecast data be used as alternate of ground meteorological parameters?. *Journal of Arid Environments*, *74*(12), 1587-1596.

Fooladmand, H. R., & Haghighat, M. (2007). Spatial and temporal calibration of Hargreaves equation for calculating monthly ETo based on Penman-Monteith method. *Irrigation and Drainage*, *56*(4), 439-449.

Fridedman, J. H. (1991). Multivariate adaptive regression splines (with discussion). *Annals of Statistics, 19*(1), 79-141.

Genuer, R., Poggi, J. M., & Tuleau-Malot, C. (2010). Variable selection using random forests. *Pattern Recognition Letters*, *31*(14), 2225-2236.

Gong, L., Xu, C. Y., Chen, D., Halldin, S., & Chen, Y. D. (2006). Sensitivity of the Penman–Monteith reference evapotranspiration to key climatic variables in the Changjiang (Yangtze River) basin. *Journal of Hydrology, 329*(3), 620-629.

González-Camacho, J. M., Cervantes-Osornio, R., Ojeda-Bustamante, W., & López-Cruz, I. (2008). Predicción de la evapotranspiración de referencia mediante redes neuronales artificiales.

Hapfelmeier, A., & Ulm, K. (2013). A new variable selection approach using random forests. *Computational Statistics & Data Analysis*, *60*, 50-69.

Hargreaves, G. H., & Samani, Z. A. (1985). Reference crop evapotranspiration from temperature. *Applied engineering in agriculture, 1*(2), 96-99.

Hofstede, R., Segarra, P., & Mena, P. (2003). Los Páramos del Mundo. Global Peatland Initiative/NC-IUCN/EcoCiencia, Quito

Irmak, S., Irmak, A., Allen, R. G., & Jones, J. W. (2003). Solar and net radiation-based equations to estimate reference evapotranspiration in humid climates. *Journal of irrigation and drainage engineering*, *129*(5), 336-347.

Jabloun, M. D., & Sahli, A. (2008). Evaluation of FAO-56 methodology for estimating reference evapotranspiration using limited climatic data: Application to Tunisia. *Agricultural water management*, *95*(6), 707-715.

Jensen, M. E., & Haise, H. R. (1963). Estimating evapotranspiration from solar radiation. Proceedings of the American Society of Civil Engineers, *Journal of the Irrigation and Drainage Division, 89*, 15-41.

Jones, J. W. & Ritchie, J. T. (1990). Crop growth models. Management of farm irrigation systems. In: Hoffman GJ, Howel TA, Solomon KH (eds), ASAE Monograph No. 9, ASAE, St. Joseph, Mich. pp. 63-89.

Khoshravesh, M., Sefidkouhi, M. A. G., & Valipour, M. (2017). Estimation of reference evapotranspiration using multivariate fractional polynomial, Bayesian regression, and robust regression models in three arid environments. *Applied Water Science*, *7*(4), 1911-1922.

Kisi, O. (2013). Least squares support vector machine for modeling daily reference evapotranspiration. *Irrigation science*, *31*(4), 611-619.

Kisi, O. (2016). Modeling reference evapotranspiration using three different heuristic regression approaches. *Agricultural Water Management*, *169*, 162-172.

Koleyni, K. (2009). Using artificial neural networks for income convergence. *Global Journal of Business Research, 3*(2), 141-152.

Kumar, M., Raghuwanshi, N. S., Singh, R., Wallender, W. W., & Pruitt, W. O. (2002). Estimating evapotranspiration using artificial neural network. *Journal of Irrigation and Drainage Engineering*, *128*(4), 224-233.

Laaboudi, A., Mouhouche, B., & Draoui, B. (2012). Neural network approach to reference evapotranspiration modeling from limited climatic data in arid regions. *International journal of biometeorology, 56*(5), 831-841.

Landeras, G., Ortiz-Barredo, A., & López, J. J. (2008). Comparison of artificial neural network models and empirical and semi-empirical equations for daily reference evapotranspiration estimation in the Basque Country (Northern Spain). *Agricultural water management*, *95*(5), 553-565.

Liu, X., Xu, C., Zhong, X., Li, Y., Yuan, X., & Cao, J. (2017). Comparison of 16 models for reference crop evapotranspiration against weighing lysimeter measurement. *Agricultural Water Management*, *184*, 145-155.

Lu, J., Sun, G., McNulty, S. G., & Amatya, D. M. (2005). A comparison of six potential evapotranspiration methods for regional use in the southeastern United States. *JAWRA Journal of the American Water Resources Association, 41*(3), 621-633.

Luteyn, J. L. (1992). Páramos: why study them? In: Balslev, H., Luteyn, J.L. (Eds.), Páramo: an Andean ecosystem under human influence. Academic Press, London, pp. 1–14

Mahringer, W. (1970). Verdunstungsstudien am neusiedler see. Arch Met Geoph Biokl Ser B, 18, 1-20. doi: 10.1007/BF02245865

Makkink, G. F. (1957). Testing the Penman formula by means of lysimeters. *Journal of the Institution of Water Engineers, 11*, 277-288.

Masters, T. (1995). *Advanced algorithms for neural networks: a C++ sourcebook*. John Wiley & Sons, Inc.

McCloud, D. E. (1955). Water requirements of field crops in Florida as influenced by climate. *Proceedings - Soil and Crop Science Society of Florida, 15*, 165-172.

Medina, G., & Mena, V. P. (2001). Los páramos en el Ecuador. *Particularidades, Problemas y Perspectivas. Proyecto Páramo. Quito. Fundación Ecuatoriana de Estudios Ecológicos*.

Mehdizadeh, S., Saadatnejadgharahassanlou, H., & Behmanesh, J. (2017). Calibration of Hargreaves–Samani and Priestley–Taylor equations in estimating reference evapotranspiration in the Northwest of Iran. *Archives of Agronomy and Soil Science*, *63*(7), 942-955.

Padrón, R. (2013). Análisis de la estructura de la lluvia del páramo. (Bachelor's thesis). Universidad de Cuenca.

Penman, H. (1948). Natural evaporation from open water, bare soil and grass. *In Proceedings of the Royal Society of London, Mathematical, Physical and Engineering Sciences, 193*(1032), 120-145.

Poulenard, J., Podwojewski, P., Janeau, J. L., & Collinet, J. (2001). Runoff and soil erosion under rainfall simulation of Andisols from the Ecuadorian Páramo: effect of tillage and burning. *Catena*, *45*(3), 185-207.

Priestley, C. H. B., & Taylor, R. J. (1972). On the assessment of surface heat flux and evaporation using large-scale parameters. *Monthly weather review, 100*(2), 81-92.

Rangel, C. (2000). La región de vida paramuna. Colombia Diversidad Biótica III. Universidad Nacional de Colombia, Instituto de Ciencias Naturales, Bogotá.

Rijtema, P. E. (1968). Derived meteorological data: transpiration. Derived Meteorological data: Transpiration. *Proceedings of the Symposium on Agroclimatological Methods*, Paris (1966).

Rohwer, C. (1931). Evaporation from free water surface. USDA Tech Null, 217, 1-96.

Samaras, D. A., Reif, A., & Theodoropoulos, K. (2014). Evaluation of radiation-based reference evapotranspiration models under different Mediterranean climates in central Greece. *Water resources management, 28*(1), 207-225.

Sánchez-Molina, J., & Poveda-Jaramillo, G. (2006). Aplicación de los métodos MARS, HOLT-WINTERS y ARIMA Generalizado en el pronóstico de caudales medios mensuales en ríos de Antioquia. *Metereología Colombiana*, *10*, 36-46.

Sandri, M., & Zuccolotto, P. (2006). Variable selection using random forests. In Data analysis, classification and the forward search (pp. 263-270). Springer Berlin Heidelberg.

Schendel U. (1967). Vegetationswasserverbrauch und -wasserbedarf. Habilitation, Kiel, 137.

Sentelhas, P. C., Gillespie, T. J., & Santos, E. A. (2010). Evaluation of FAO Penman–Monteith and alternative methods for estimating reference evapotranspiration with missing data in Southern Ontario, Canada. *Agricultural Water Management, 97*(5), 635-644.

Shiri, J. (2017). Evaluation of FAO56-PM, empirical, semi-empirical and gene expression programming approaches for estimating daily reference evapotranspiration in hyper-arid regions of Iran. *Agricultural Water Management*, *188*, 101-114.

Singh, V. P., & Xu, C. Y. (1997). Evaluation and generalization of 13 mass-transfer equations for determining free water evaporation. *Hydrological Processes, 11*(3), 311-323.

Strobl, C., Boulesteix, A. L., Kneib, T., Augustin, T., & Zeileis, A. (2008). Conditional variable importance for random forests. *BMC bioinformatics*, *9*(1), 307.

Strobl, C., Boulesteix, A. L., Zeileis, A., & Hothorn, T. (2007). Bias in random forest variable importance measures: Illustrations, sources and a solution. *BMC bioinformatics*, *8*(1), 25.

Tabari, H., & Talaee, P. H. (2011). Local calibration of the Hargreaves and Priestley-Taylor equations for estimating reference evapotranspiration in arid and cold climates of Iran based on the Penman-Monteith model. *Journal of Hydrologic Engineering*, *16*(10), 837-845.

Tabari, H., Grismer, M. E., & Trajkovic, S. (2013). Comparative analysis of 31 reference evapotranspiration methods under humid conditions. *Irrigation Science, 31*(2), 107-117.

Trabert, W. (1896). Neue Beobachtungen über Verdampfungsgeschwindigkeiten. Meteorol Z., 13, 261-263.

Trajkovic, S., & Kolakovic, S. (2009). Estimating reference evapotranspiration using limited weather data. *Journal of irrigation and drainage engineering*, *135*(4), 443-449.

Trajkovic, S., Todorovic, B., & Stankovic, M. (2003). Forecasting of reference evapotranspiration by artificial neural networks. *Journal of Irrigation and Drainage Engineering*, *129*(6), 454-457.

Traore, S., Wang, Y. M., & Kerh, T. (2010). Artificial neural network for modeling reference evapotranspiration complex process in Sudano-Sahelian zone. *Agricultural water management, 97*(5), 707-714.

Turc, L. (1961). Estimation of irrigation water requirements, potential evapotranspiration: a simple climatic formula evolved up to date. *Annals of Agronomy, 12*(1), 13-49.

Valiantzas, J. D. (2013). Simplified forms for the standardized FAO-56 Penman–Monteith reference evapotranspiration using limited weather data. *Journal of hydrology, 505*, 13-23.

Valipour, M. (2015). Temperature analysis of reference evapotranspiration models. *Meteorological Applications*, *22*(3), 385-394.

Valipour, M. (2017). Calibration of mass transfer-based models to predict reference crop evapotranspiration. *Applied Water Science*, *7*(2), 625-635.

Velásquez-Henao, J. D., Franco-Cardona, C. J., & Camacho, P. A. (2014). Nonlinear time series forecasting using MARS. *Dyna*, *81*(184), 11-19.

Verstraeten, W. W., Veroustraete, F., & Feyen, J. (2008). Assessment of evapotranspiration and soil moisture content across different scales of observation. *Sensors, 8*(1), 70-117.

World Meteorological Organization (WMO) (1966). Measurement and estimation of evaporation and evapotranspiration. Tech Pap. (CIMO-Rep) 83. Genf.

Xu, C. Y., & Singh, V. P. (2002). Cross comparison of empirical equations for calculating potential evapotranspiration with data from Switzerland. *Water Resources Management, 16*(3), 197-219.

Yoder, R. E., Odhiambo, L. O., & Wright, W. C. (2005). Evaluation of methods for estimating daily reference crop evapotranspiration at a site in the humid southeast United States. *Applied engineering in agriculture*, *21*(2), 197-202.

Appendix 1: Daily ETo estimations of temperature-based models. Temporal comparison against the reference model (FAO 56 P-M) for both weather stations.

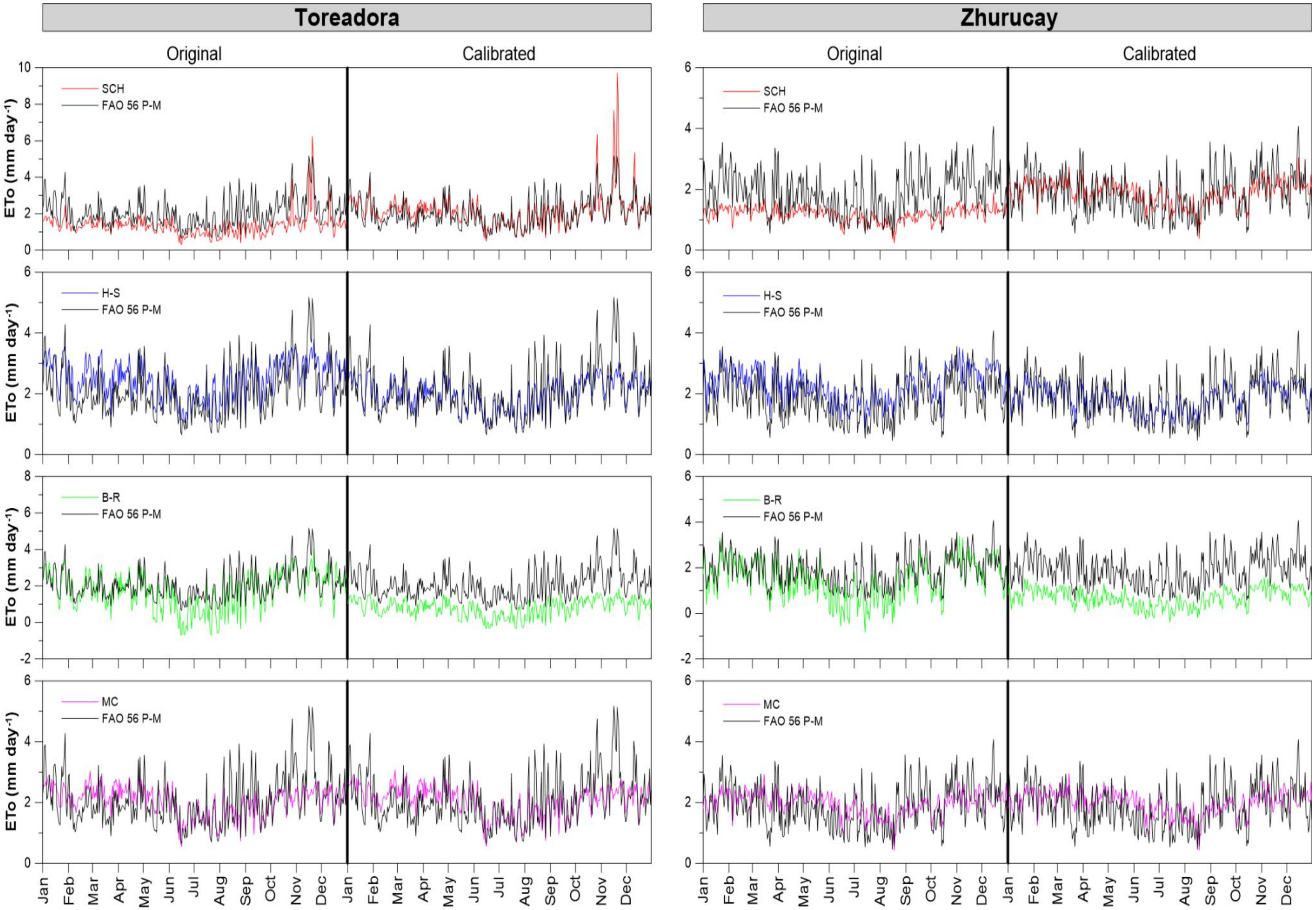

Appendix 2: Daily ETo estimations of radiation-based models. Temporal comparison against the reference model (FAO 56 P-M) for Toreadora weather station.

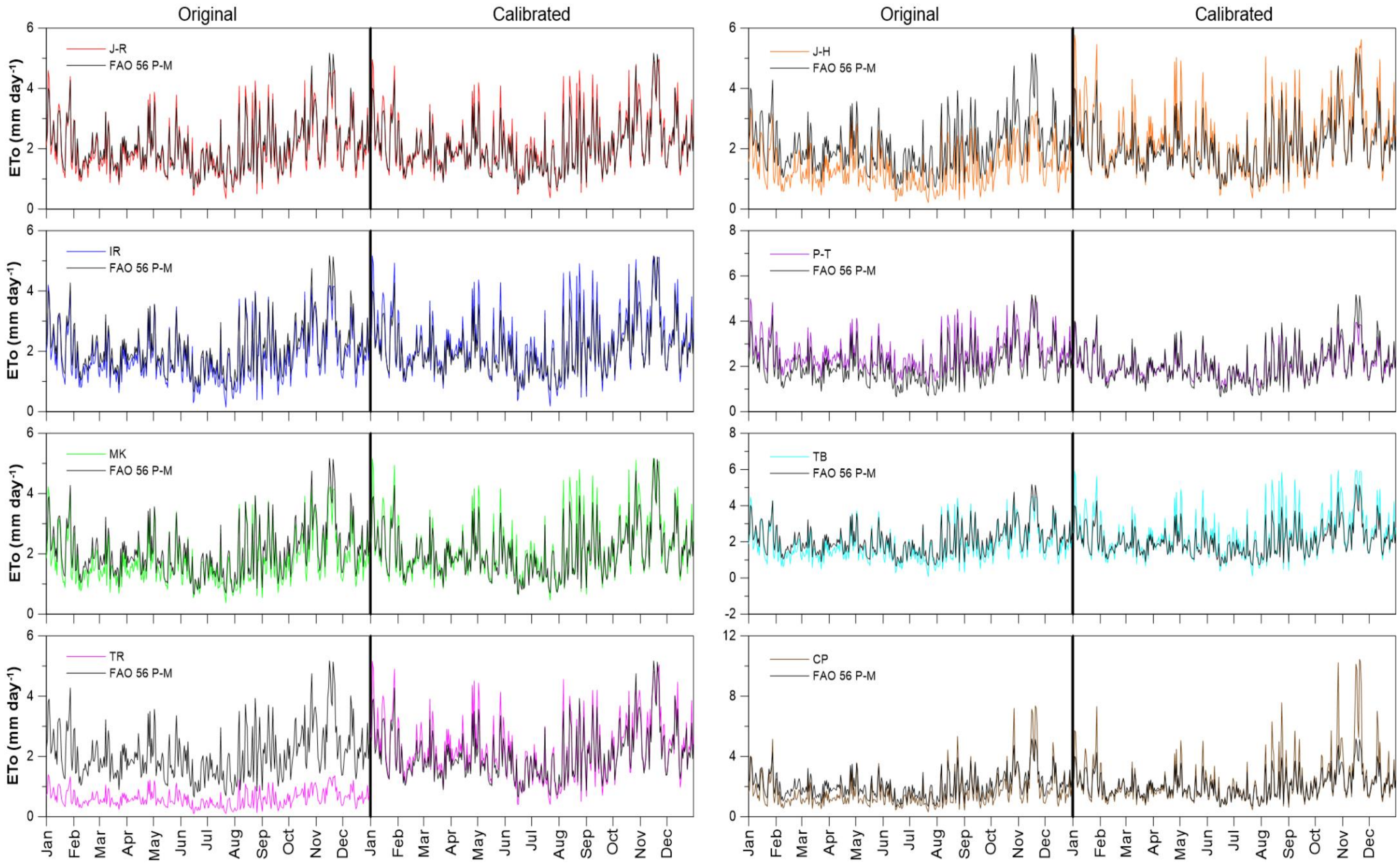

Appendix 3: Daily ETo estimations of radiation-based models. Temporal comparison against the reference model (FAO 56 P-M) for Zhurucay weather station.

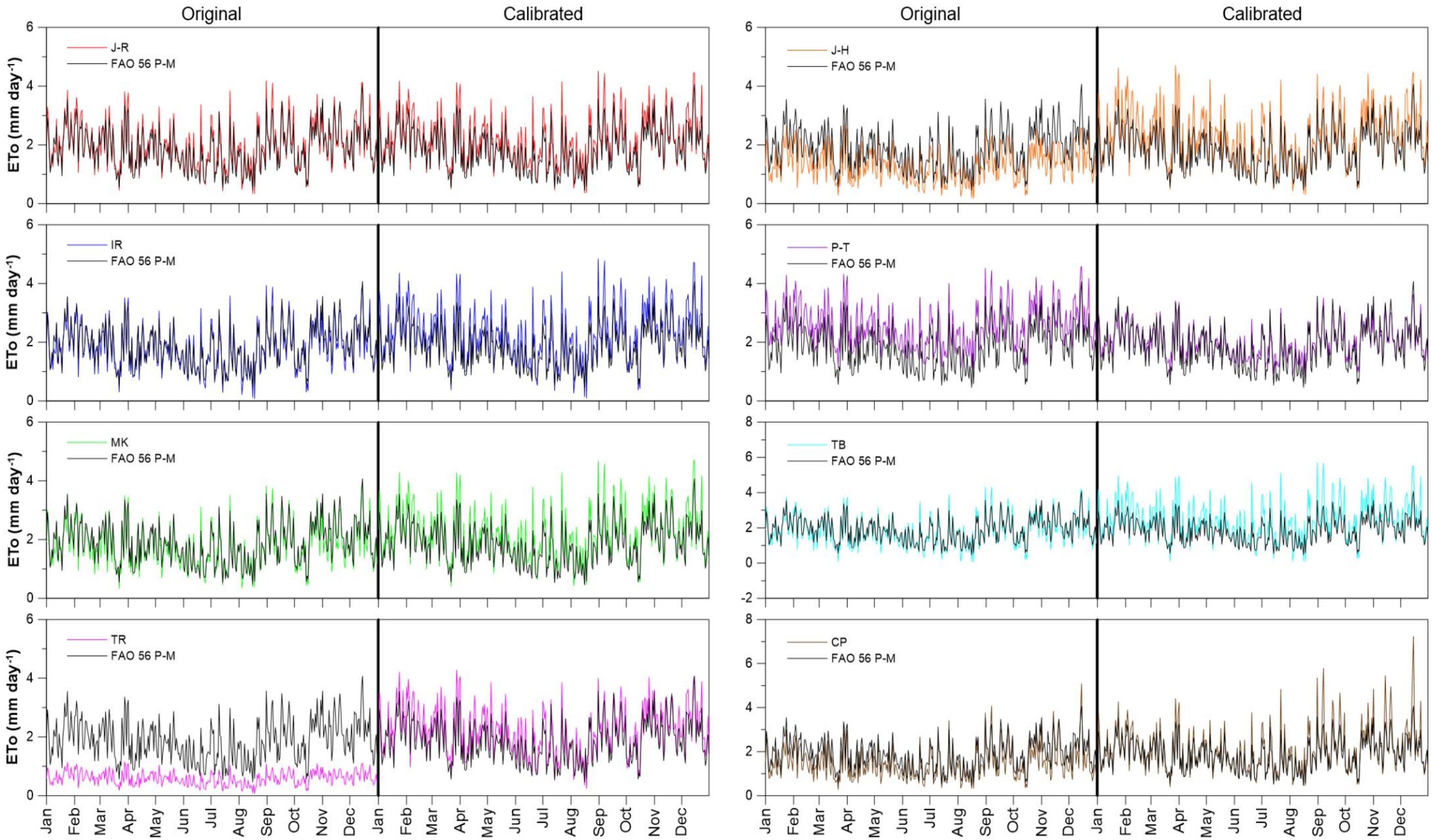

Appendix 4: Daily ETo estimations of combination-based models. Temporal comparison against the reference model (FAO 56 P-M) for both weather stations.

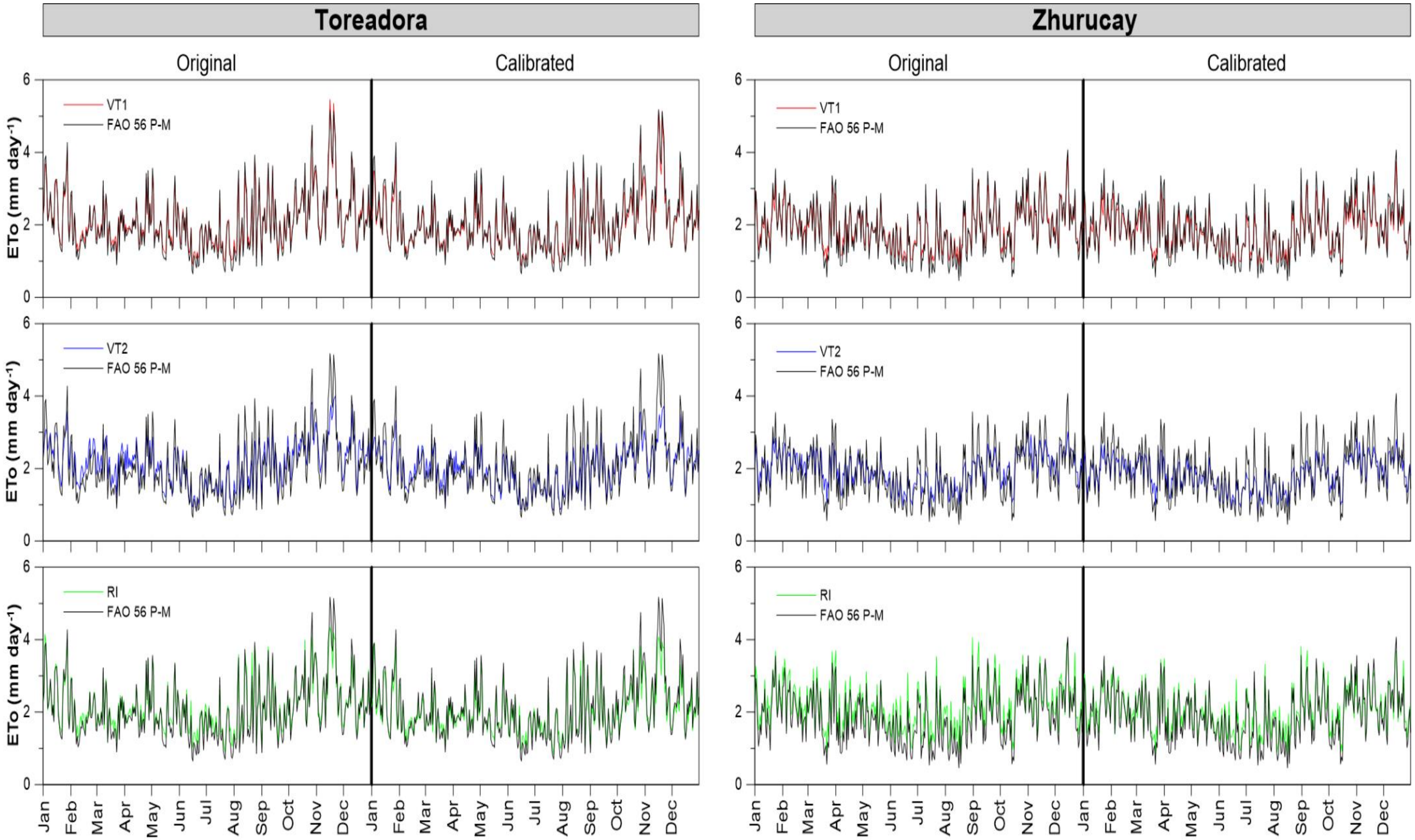

Appendix 5: Daily ETo estimations of mass transfer-based models. Temporal comparison against the reference model (FAO 56 P-M) for Toreadora weather station.

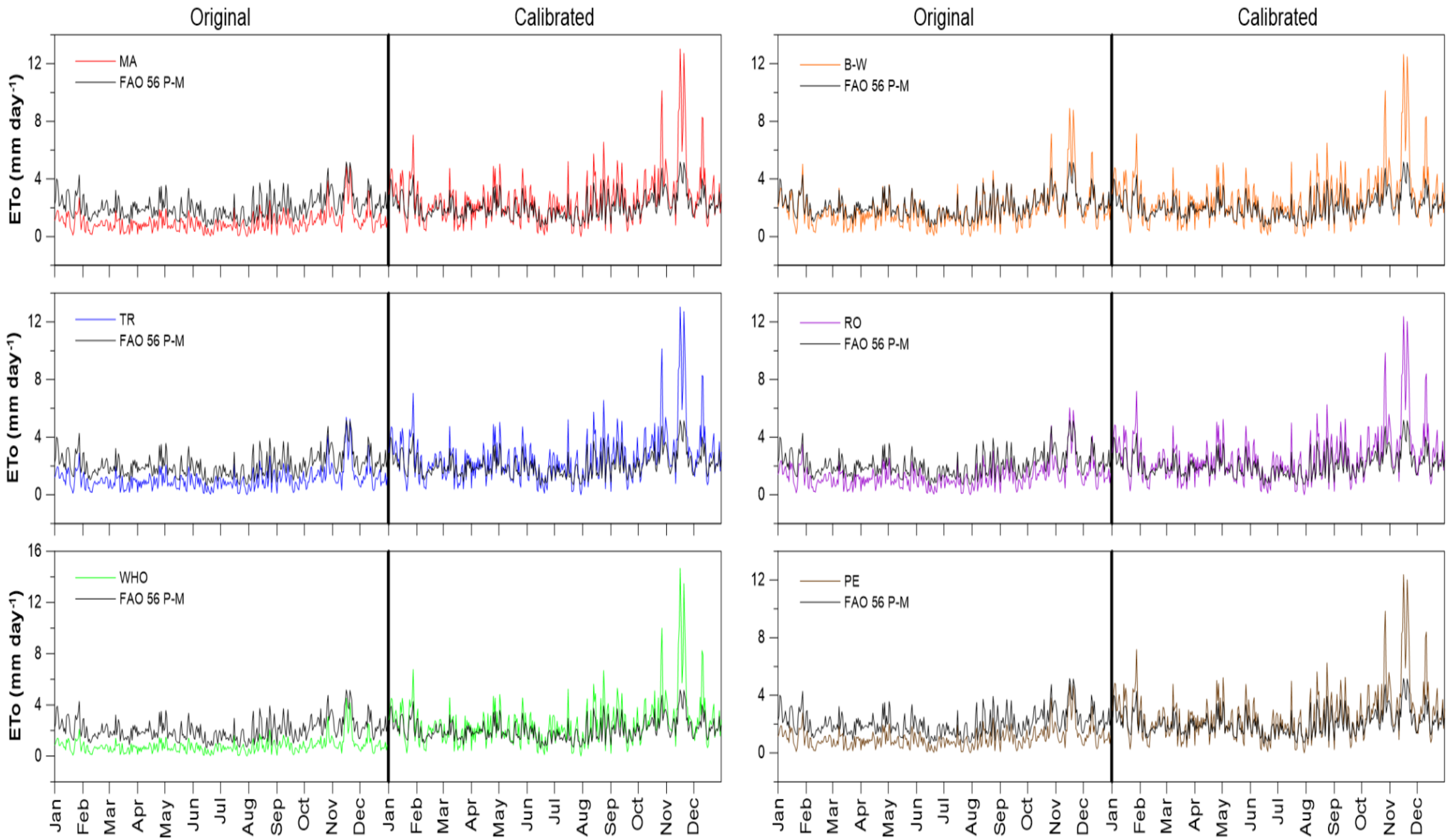

Appendix 6: Daily ETo estimations of mass transfer-based models. Temporal comparison against the reference model (FAO 56 P-M) for Zhurucay weather station.

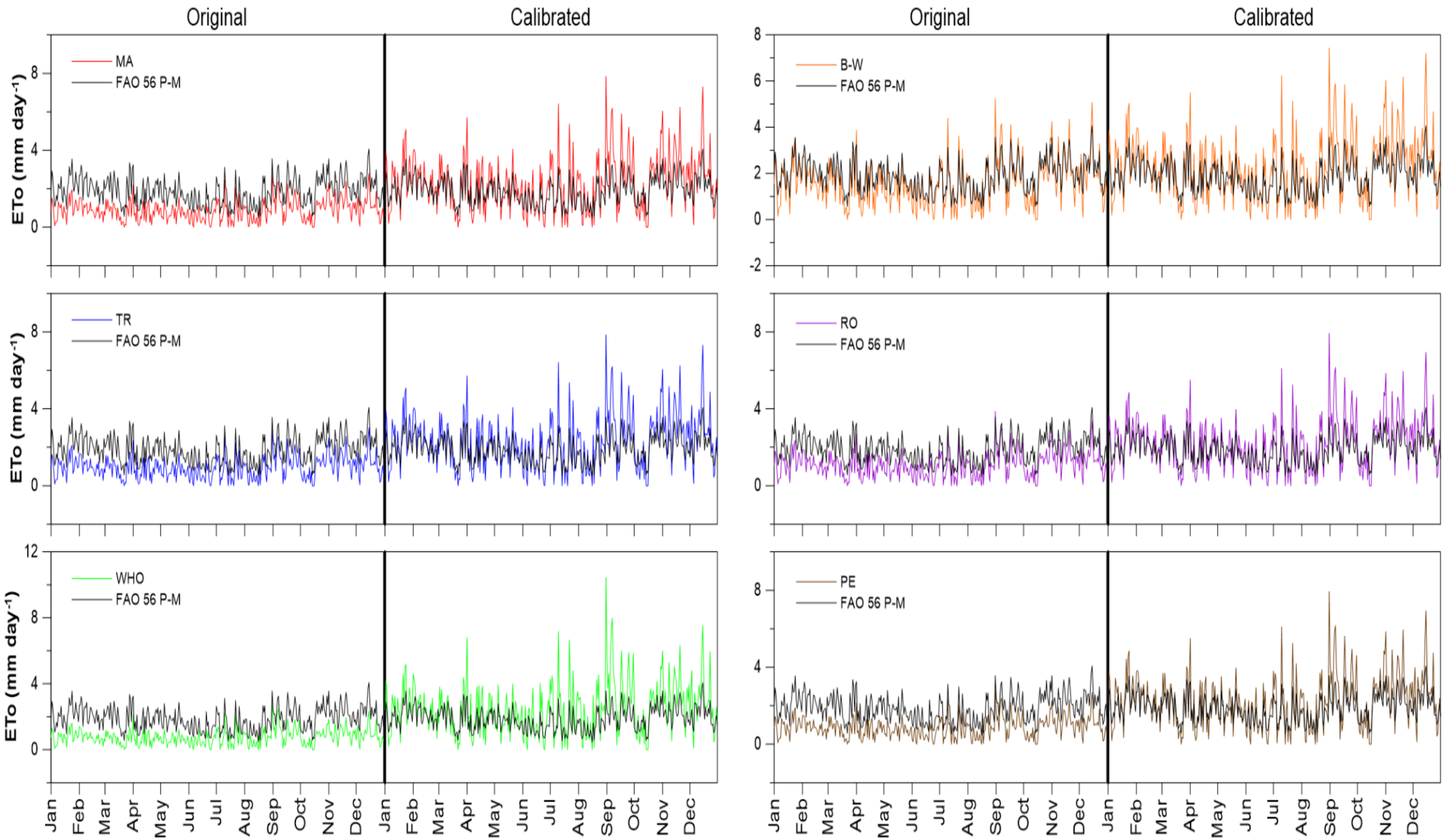

Appendix 7: Daily ETo estimations of ANN models. Temporal comparison against the reference model (FAO 56 P-M) for Toreadora weather station.

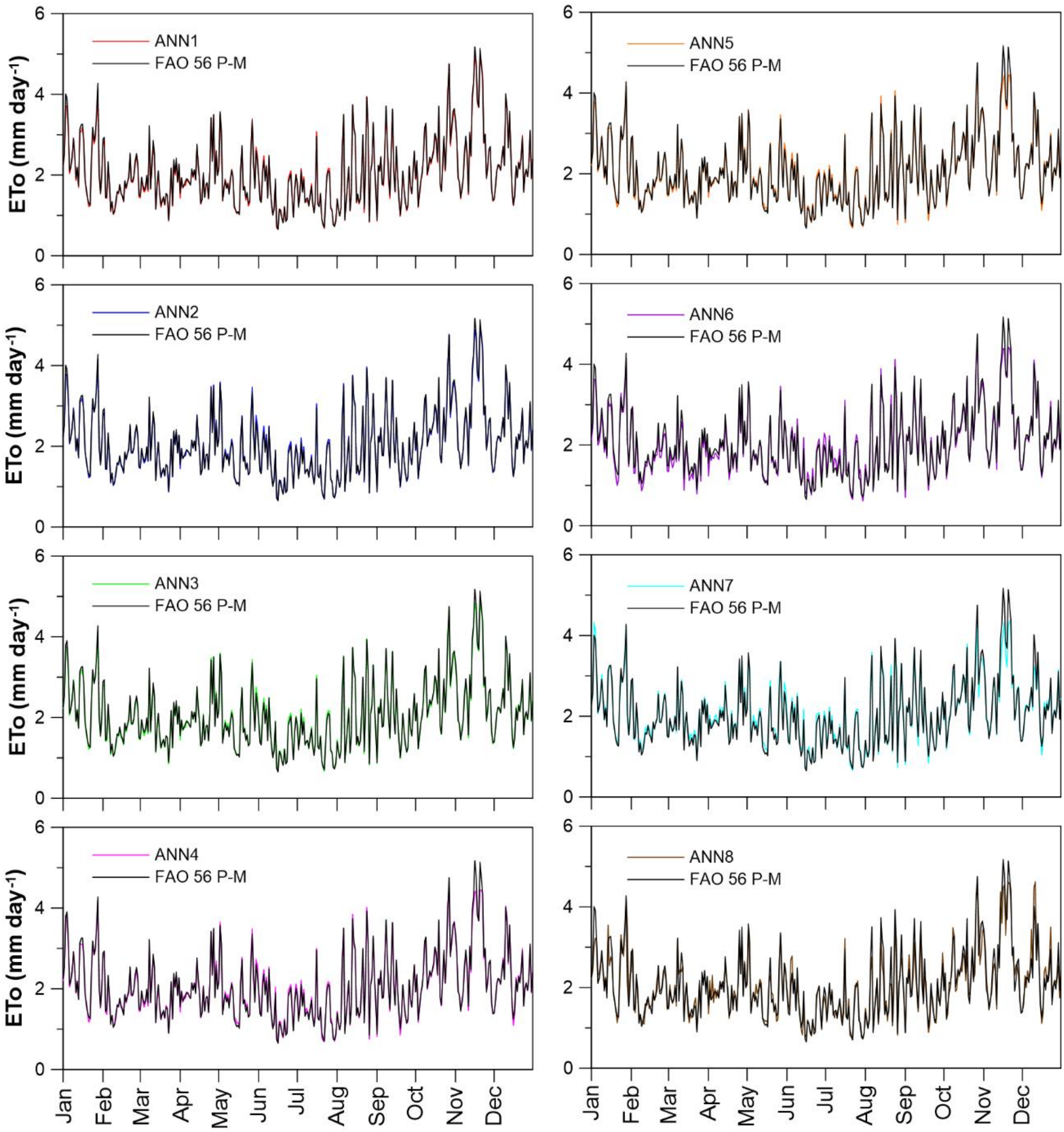

Appendix 8: Daily ETo estimations of ANN models. Temporal comparison against the reference model (FAO 56 P-M) for Zhurucay weather station.

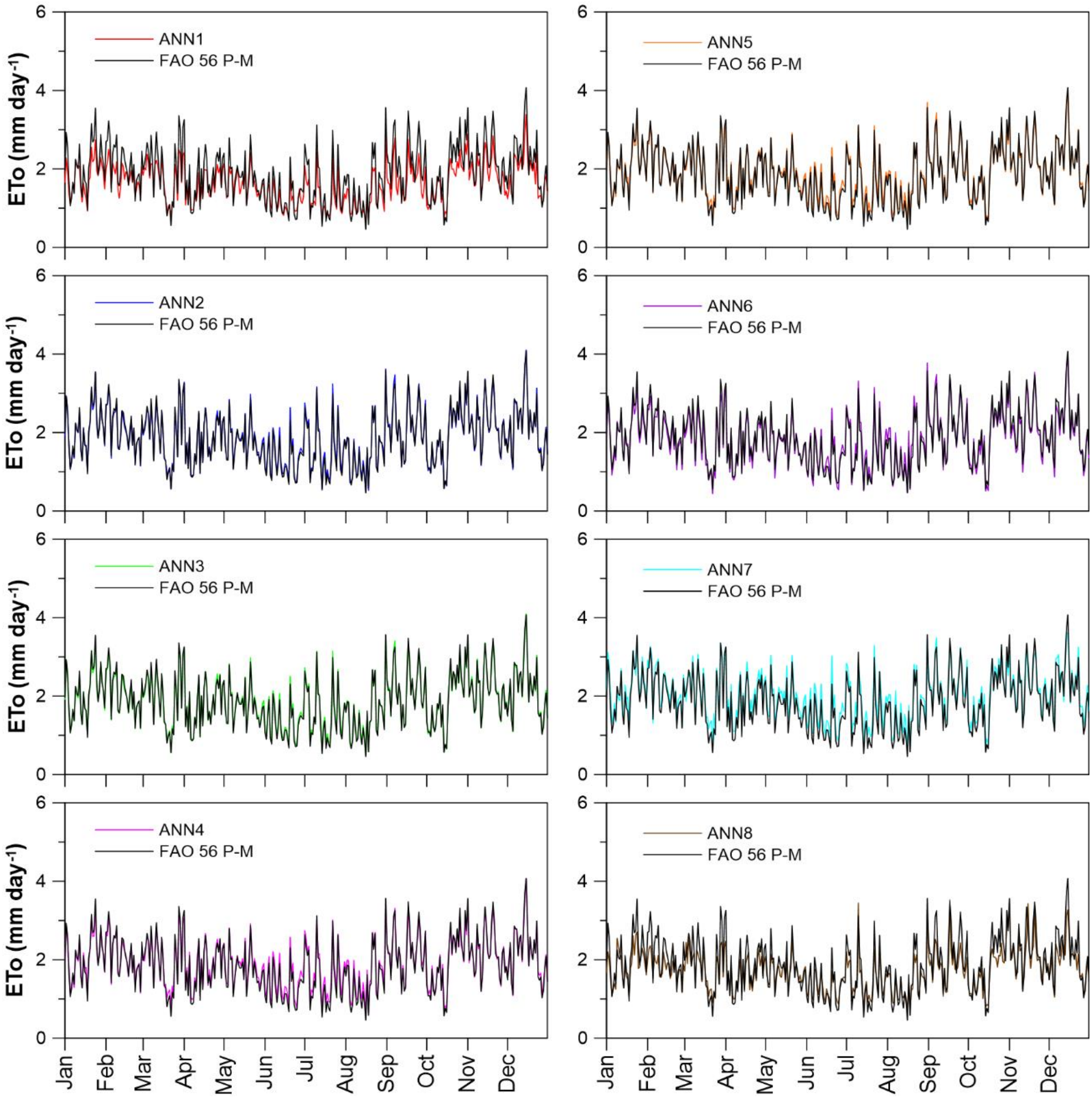

Appendix 9: Daily ETo estimations of REMPE model. Temporal comparison against the reference model (FAO 56 P-M) for both weather stations.

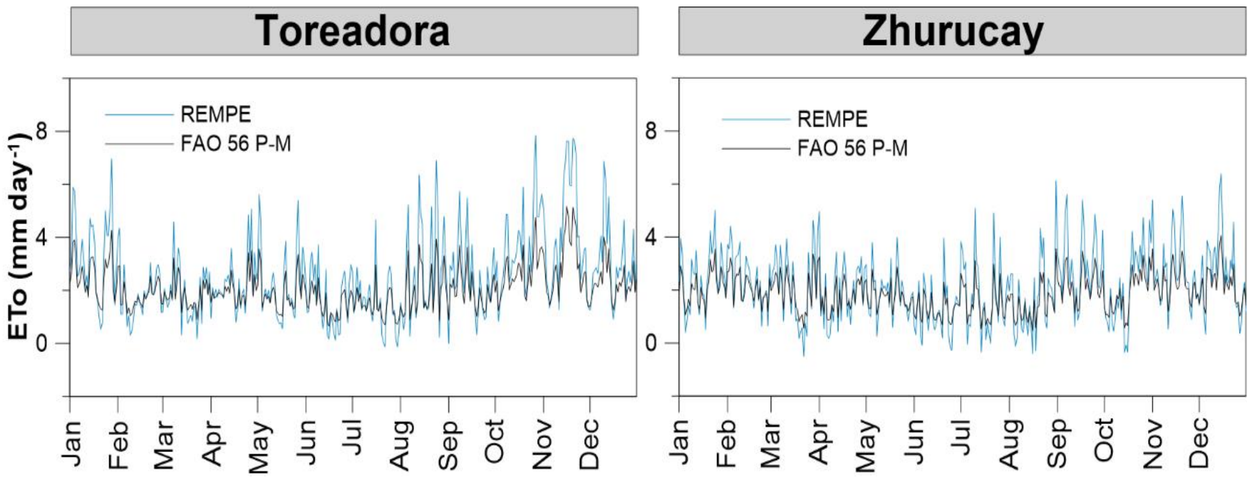

Appendix 10. Statistical performance of ETo estimation methods *versus* FAO 56 P-M model for daily ETo estimation with data from the 2016 period (Toreadora weather station).

Model	Type	MBE (mm)	MAE (mm)	RMSE (mm)	cr		MBE (mm)	MAE (mm)	RMSE (mm)
Original							Calibrated		
SCH	Temperature-based	-0.74	0.75	0.89	1,62		0.089	0.38	0.58
H-S		0.42	0.56	0.64	0,80		-0.078	0.32	0.51
B-R		-0.32	0.50	0.67	0,46		-1.270	1.27	1.37
MC		-0.04	0.49	0.68	1,01		-0.016	0.50	0.68
J-R	Radiation-based	-0.07	0.16	0.21	1,08		0.087	0.17	0.25
IR		-0.25	0.26	0.30	1,23		0.176	0.24	0.34
MK		-0.30	0.31	0.35	1,22		0.096	0.20	0.29
TR		-1.47	1.47	1.58	3,69		0.166	0.24	0.31
J-H		-0.74	0.74	0.77	1,73		0.242	0.33	0.45
P-T		0.48	0.48	0.51	0,79		-0.058	0.17	0.24
TB		-0.27	0.32	0.36	1,32		0.305	0.39	0.57
CP		-0.42	0.54	0.61	1,42		0.275	0.43	0.92
VT1	Combination-based	0.05	0.10	0.12	0,95		-0.059	0.12	0.16
VT2		0.10	0.30	0.39	0,93		-0.054	0.27	0.40
RI		0.07	0.14	0.20	0,94		-0.059	0.16	0.23
MA	Mass transfer-based	-1.07	1.07	1.11	2,60		0.546	0.76	1.22
TR		-0.99	0.99	1.04	2,42		0.548	0.76	1.22
WMO		-1.27	1.27	1.33	3,23		0.525	0.74	1.26
B-W		-0.22	0.44	0.63	1,42		0.561	0.77	1.22
RO		-0.79	0.80	0.84	2,05		0.566	0.77	1.19
PE		-1.05	1.05	1.09	2,57		0.565	0.76	1.19
ANN1	Artificial Neural Networks	-	-	-	-		-0.025	0.04	0.06
ANN2		-	-	-	-		-0.007	0.04	0.05
ANN3		-	-	-	-		-0.009	0.04	0.06
ANN4		-	-	-	-		-0.010	0.06	0.09
ANN5		-	-	-	-		-0.011	0.05	0.09

ANN6		-	-	-	-		-0.038	0.10	0.13
ANN7		-	-	-	-		-0.001	0.09	0.15
ANN8		-	-	-	-		-0.016	0.18	0.27
REMPE	MARS	-	-	-	-		0.493	0.67	0.93

Appendix 11. Statistical performance of ETo estimation methods versus FAO 56 P-M model for daily ETo estimation with data from the 2014 period (Zhurucay weather station).

Model	Type	MBE (mm)	MAE (mm)	RMSE (mm)		MBE (mm)	MAE (mm)	RMSE (mm)
Original						**Calibrated**		
SCH	Temperature-based	-0.70	0.72	0.90		0.020	0.41	0.50
H-S		0.46	0.52	0.57		-0.008	0.29	0.38
B-R		-0.38	0.47	0.57		-1.188	1.19	1.25
MC		0.10	0.49	0.60		0.119	0.50	0.60
J-R	Radiation-based	0.12	0.18	0.24		0.274	0.30	0.37
IR		-0.06	0.15	0.20		0.362	0.39	0.47
MK		-0.10	0.17	0.22		0.285	0.31	0.40
TR		-1.28	1.28	1.37		0.314	0.34	0.40
J-H		-0.57	0.57	0.62		0.374	0.40	0.50
P-T		0.67	0.67	0.69		0.137	0.20	0.24
TB		-0.07	0.21	0.27		0.505	0.55	0.70
CP		-0.41	0.43	0.47		0.202	0.28	0.47
VT1	Combination-based	0.04	0.13	0.16		-0.052	0.15	0.19
VT2		0.09	0.30	0.36		-0.047	0.28	0.37
RI		0.28	0.29	0.32		0.151	0.19	0.23
MA	Mass transfer-based	-0.99	0.99	1.03		0.435	0.69	0.92
TR		-0.92	0.92	0.96		0.436	0.69	0.92
WMO		-1.10	1.10	1.17		0.613	0.85	1.19
B-W		-0.28	0.42	0.50		0.393	0.65	0.86
RO		-0.79	0.79	0.84		0.349	0.62	0.84
PE		-1.01	1.01	1.05		0.350	0.62	0.84
ANN1	Artificial Neural Networks	-	-	-		-0.25	0.28	0.36
ANN2		-	-	-		0.012	0.05	0.07
ANN3		-	-	-		0.010	0.05	0.06
ANN4		-	-	-		0.046	0.09	0.11
ANN5		-	-	-		0.040	0.08	0.10

ANN6		-	-	-		-0.023	0.11	0.13
ANN7		-	-	-		0.141	0.17	0.20
ANN8		-	-	-		-0.144	0.24	0.32
REMPE	MARS	-	-	-		0.292	0.55	0.71